

# The thermal and geodynamic evolution of the Lapland granulite belt: Implications for thermal structure of the lower crust during granulite-facies metamorphism

Michael V. Mints<sup>a,\*</sup>, Tatiana V. Kaulina<sup>b</sup>, Alexander N. Konilov<sup>a</sup>,  
Alexander V. Krotov<sup>c</sup>, Vladimir M. Stupak<sup>d</sup>

<sup>a</sup> Geological Institute, RAS, Moscow, Russia

<sup>b</sup> Geological Institute, Kola Sci. Center of RAS, Apatity, Murmansk region, Russia

<sup>c</sup> Moscow State University, Moscow, Russia

<sup>d</sup> SPETSGEOPHYSICA, Povarovka, Moscow region, Russia

Received 30 October 2005; accepted 18 October 2006

Available online 21 December 2006

## Abstract

The tectono-thermal history of the Lapland Granulite belt is considered within the framework of a combined superplume-plate tectonic model on the basis of new geochronological and petrological data. The high-grade metamorphic events were linked with plume-related extensional episodes at ~2.44 Ga (M0), ~2.0–1.95 Ga (M1), ~1.95–1.92 Ga (M2) and 1.92–1.91 Ga (M3). The last (M4) high-grade event at ~1.89–1.87 Ga corresponds to the final collision. *P–T* parameters of metamorphism during M1 event ranged from 960 to 860 °C and from 14.0 to 10.3 kbar. They decreased from the lower to the upper part of the belt during the M2 event from 860 °C at 12.4 kbar and to 800 °C at 5.8 kbar, during the M3 event from 770 °C at 10.7 kbar to 640 °C at 4.8 kbar, and during the M4 event from 650 °C at 8.4 kbar to 550 °C at 4.5 kbar. Upward displacement of a hot tectonic slice during the M4 stage caused inverted metamorphic zoning in the autochthonous rocks and a clockwise *P–T* evolution within the mélangé zone at the base of LGB<sup>1</sup>. The internal thermal gradient within the lower crust during events M2 and M3 was 1.8–2.3 °C/km, and during the M4 event it fell to 4–5 °C/km. The agreement of thickness estimates of the granulite ensemble obtained from seismic and petrological data attests to the lithostatic nature of metamorphic pressures. The average thickness of the Lapland granulite slice was initially ~21–23 km.

© 2006 International Association for Gondwana Research. Published by Elsevier B.V. All rights reserved.

**Keywords:** Lapland; Granulite; Crustal thermal structure; Fennoscandian shield; Geodynamic evolution; Palaeoproterozoic

## 1. Introduction

At the present time ideas on the nature and tectonic and geodynamic significance of granulite–gneiss belts remain controversial. Structural constraints indicate that many large-scale granulite terranes evolved within a broadly collisional context. However, some features of granulite–gneiss belts are in conflict with this interpretation. In particular, some data indicate that thermal gradients within the continental crust during

granulite-facies metamorphism (“internal” thermal gradients) were rather low, *ca.* 5–10 °C/km at most (*e.g.* Perchuk and Gerya, 1989; Barbey and Raith, 1990; Raith et al., 1990; Schumacher and Faulhaber, 1994; Mints and Konilov, 1998, 2004). This suggests the significant heating of not only lower, but also middle crust resulted in high temperatures and rather high *T/P* ratios in corresponding sections of the upper crust. Harley (1992) argued that collision-related lithospheric thickening is not capable of explaining very high temperatures typical of most granulites for reasonable limits on critical model parameters such as the thermal conductivity, crustal heat productivity and basal heat flux. The regional granulite metamorphism thus requires additional input of mantle heat. Harley’s arguments are especially relevant in the light of the inferred

\* Corresponding author. Tel.: +7 495 951 3020; fax: +7 495 951 0443.

E-mail address: [michael.mints@mtu-net.ru](mailto:michael.mints@mtu-net.ru) (M.V. Mints).

<sup>1</sup> Lapland Granulite Belt.

enormous thickness of some granulite-facies crustal sections. Another key factor in the formation of granulite-facies terranes is low  $a_{\text{H}_2\text{O}}$  conditions resulting in the relatively anhydrous (“dry”) mineral assemblages not only in the metasedimentary granulites but also in enderbite–charnockite magmas (Touret and Hartel, 1990). An increased water activity, which is characteristic of suprasubduction settings, causes partial melting and temperature stabilization at amphibolite-facies conditions. The regional desiccation of the crustal rocks is unlikely in the suprasubduction environment and may be linked with back-arc extension. Sandiford (1989) and Harley (1989) consider the possibility of granulite-facies metamorphism during continental rifting and suggest that granulites are forming today beneath the North American Basin and Range province.

The LGB, which is one of the best-studied tectonic units of the northeastern Fennoscandian Shield (Fig. 1), is a key area for study of the nature, tectonic and geodynamic significance of granulite–gneiss belts. Two ideas on its origin and evolution predominate. According to the first one, based mostly on geochemical and geochronological data, the LGB front represents a fossil Palaeoproterozoic subduction zone (Hörmann et al., 1980; Barbey and Raith, 1990 and references therein; Daly et al., 2001; Balagansky et al., 2001). Evolutionary models of the second type, based on the same data, focus on specific aspects of the evolution of the adjacent Pechenga–Imandra–Varzuga low-grade volcano-sedimentary belt and suggest an

origin of the LGB assemblage in a back-arc environment (Marker, 1985; Berthelsen and Marker, 1986; Melezhik and Sturt, 1994). Both types of model fail to incorporate some important details of the geological setting and metamorphic evolution of the LGB, such as (1) the uniform structural position of two generations of the gabbro–anorthosite bodies with ages of  $\sim 2.45$  and 2.1–1.9 Ga and their geodynamic significance, (2) the similar metamorphic evolution of these bodies with granulite–gneiss assemblages, and (3) the temporal and geodynamic relationships between the LGB and the Palaeoproterozoic low-grade volcano-sedimentary belts in the Kola Peninsula and Northern Karelia.

Another approach has been suggested by Gerya et al. (2000, 2001, 2002), who performed numerical modeling experiments on the geodynamic evolution (exhumation) of the LGB and some other granulite–gneiss belts. Although very attractive, this model operates with questionable boundary conditions (too heavy middle and upper crust, too light granulites and some others). Furthermore, this model bears no relationship to the regional geological structure and crustal evolution of the northeastern Fennoscandian Shield.

Recently Mints and Konilov (2004) have proposed a model for Palaeoproterozoic crustal evolution in the East European and North America cratons by emphasizing the interaction of plume- and plate tectonic-related crustal-forming processes and their role in the origin and evolution of the granulite belts.

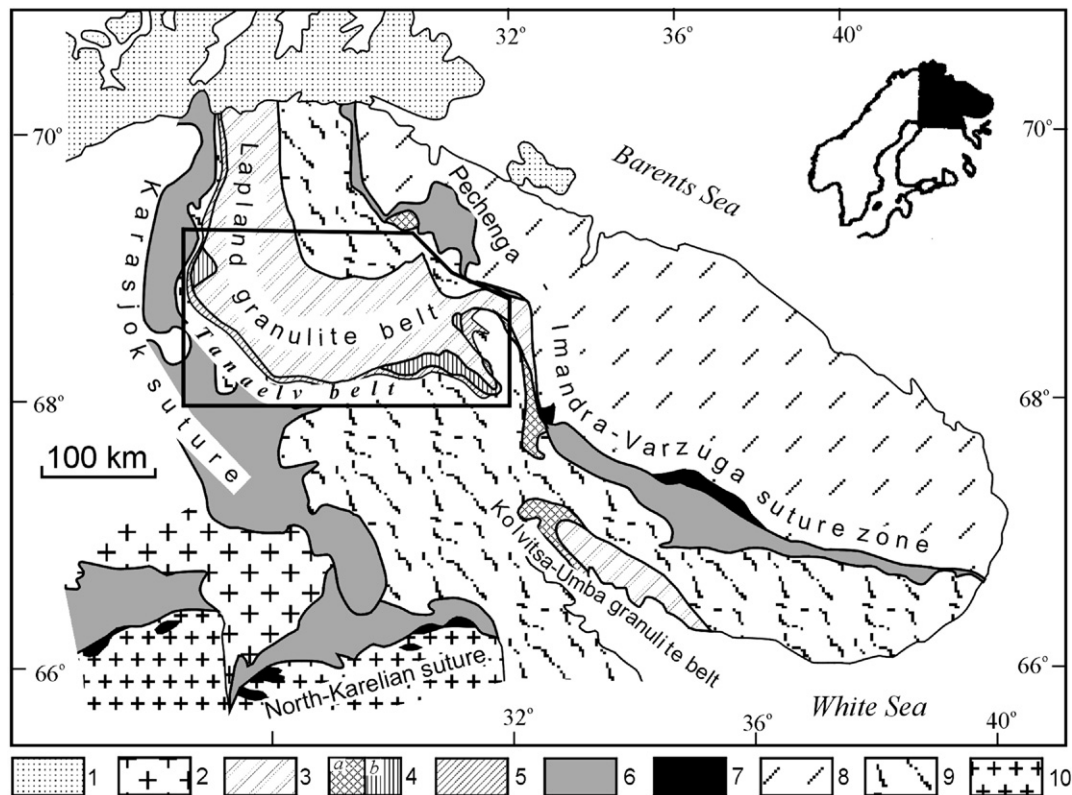


Fig. 1. Simplified geological map of the northeastern Svecofennian Shield showing the location of the Lapland granulite belt. The studied area is outlined. 1: Phanerozoic and Neoproterozoic; 2–6: Palaeoproterozoic— 2: Svekofennian (late Palaeoproterozoic) granites; 3–4: Lapland–Kolvitsa–Umba thrust nappe granulite belt— 3: granulites; 4: metagabbro–anorthosite bodies (a: first generation,  $\sim 2.45$  Ga; b: second generation, 2.1–1.9 Ga); 5: main tectonic mélangé zone (Tana or Tanaely belt, see discussion in the text); 6: volcano-sedimentary belts (sutures); 7– layered mafic–ultramafic bodies; 8–10: Archaean units— 8: Murmansk; 9: Belomorian; 10: Karelian.

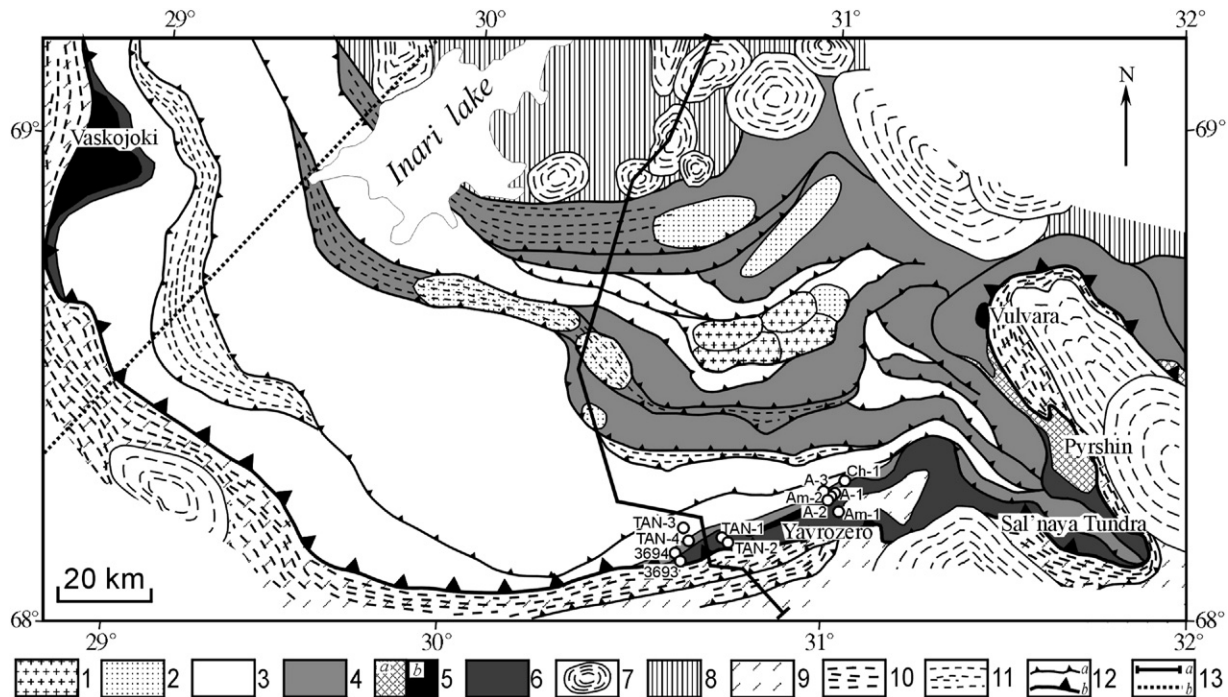


Fig. 2. Simplified geological map of the central part of the Palaeoproterozoic Lapland granulite belt. 1–6: Palaeoproterozoic Lapland complex— 1: Grt-bearing granites; 2: enderbites and Px-bearing diorites; 3: khondalites; 4: mafic granulites; 5: gabbro-anorthosites (a: first generation, ~2.45 Ga; b: second generation, 2.1–1.9 Ga); 6: metagabbro-anorthosites (Grt–Pl–Px schists and Grt amphibolites); 7: granite-gneiss and granite-migmatite domes; 8–9: autochthonous amphibolite-gneiss complexes— 8: Inari unit; 9: Belomorian belt; 10–11: tectonic mélangé zones— 10: between thrust nappe package and parautochthon; 11: within thrust nappe package; 12: main (a) and secondary (b) thrusts; 13: seismic profiles: EGGI (a) and Polar (b). The gabbro-anorthosite massifs mentioned in the text are identified. The localities of samples discussed in the text are shown.

In this paper data on the spatial distribution of  $P$ – $T$  parameters and timing of successive metamorphic events in the LGB are presented and discussed. Special emphasis is made of the metamorphic pressure–depth relationship. At present there is almost universal agreement among researchers that pressure estimates in granulite–gneiss complexes reflect the depth of metamorphism, *i.e.*, may be defined as lithostatic pressure. Accordingly, when interpreting the tectonic history of an area, the estimated pressure is converted to depth, assuming that the pressure was caused by the load of overlying rocks. However, in high-strain zones this assumption cannot be justified directly. Thus, independent ways are required to estimate the depths of tectono-metamorphic events and the significance or insignificance of tectonic overpressure. A unique opportunity to examine this problem is offered by reflection seismic profiling across the LGB that permits an estimation of the true thickness of the LGB slice and comparison with the thickness calculated from metamorphic pressures inferred for lower and upper parts of the belt.

Though many geochronological investigations have been devoted to the LGB rocks, the chronology of the metamorphic stages remained controversial. Analysis of available geochronological data set and newly performed U–Pb and Sm–Nd dating on minerals from metamorphic rocks in the lower part of the LGB have permitted us to evaluate and discuss the temporal relationships between two generations of the gabbro-anorthosite bodies, the succession of metamorphic events, and the cooling history of the LGB assemblage.

Elaboration of a model of the thermal and geodynamic evolution of the LGB based on an integration of results available from the study of metamorphic processes, petrological mapping, including the geochronological data set and reflection seismic data on the crustal structure of the LGB, is the main target of this work together with a reconstruction of the thermal structure of the lower crust during granulite-facies metamorphism.

## 2. Geology

The LGB is one of the main structures of the Palaeoproterozoic collision orogen in the northeastern Fennoscandian Shield (Fig. 1). Based on geological mapping, structural and seismic data it constitutes a thrust nappe ensemble (Gaál et al., 1989; Barbey and Raith, 1990 and references therein; Marker et al., 1990; Mints et al., 1996). The LGB is formed by three main types of lithological and igneous assemblages (Fig. 2). The first one contains mafic granulites (Opx–Cpx–Pl— in some cases Grt-bearing gneisses<sup>2</sup>) and related enderbite bodies. Hbl-bearing mafic granulites alternating with Px-bearing amphibolites are characteristic of the northern part of the belt accompanied by Px-bearing diorite bodies. Assemblage of the second type is made up of felsic granulites and khondalites (metasediments), which are mainly Grt–Sil, Grt–Cor–Sil and Grt–Sil–Bt gneisses and also Grt-bearing tonalites, granites and plagiogranites having sharp or gradual contacts with the metamorphic rocks; small

<sup>2</sup> Here and below mineral abbreviations are after Kretz (1983).

calc-silicate lenses occur locally. The third type assemblage comprises plagioclases (metaanorthosites) with gradual transitions to Grt–Cpx–Pl schists (metagabbro–anorthosites) and underlying garnet amphibolites (metagabbro) (Mints et al., 1996). Plate-shaped bodies formed by the latter assemblage are exposed at the base of the thrust package. Geochronological data have revealed that layered gabbro–anorthosite bodies belong to two generations with ages of ~2.45 and 2.1–1.9 Ga (see Figs. 1 and 2). The thrust nappe ensemble is underlain by a tectonic mélange zone, named the West Inari schist zone (Meriläinen, 1976), Tana (Barbey et al., 1980) or Tanaelv belt (Krill, 1985). It is formed of kyanite-bearing garnet-biotite schists and amphibolites and contains tectonically bounded layers and lenses of LGB granulite-facies rocks (metaanorthosites, garnet amphibolites and mafic granulites). An inverted metamorphic zoning from amphibolite to epidote–amphibolite facies has been recognized in this zone (Hörmann et al., 1980; Barbey and Raith, 1990; Mints et al., 1996, Perchuk et al., 1999).

It is commonly suggested that the layered gabbro–anorthosite bodies are a part of the mélange zone (e.g., Balagansky et al., 2001; Daly et al., 2001). However, intrusive contacts with hosted mafic granulites (e.g., Marker et al., 1999), emplacement of two distinct gabbro–anorthosite generations in the same tectonic position and their mutual metamorphic history with the granulitic assemblages (as shown below) strongly indicate that layered gabbro–anorthosite bodies form a part of the Lapland granulite complex proper. The term “Tanaelv belt” may be used for the sheared moderate-grade volcano-sedimentary assemblage with inverted metamorphic zoning localized between the LGB and the underlying Belomorian rocks.

### 3. Petrological ( $P$ – $T$ ) mapping

#### 3.1. Thermobarometry and pressure–temperature relationships

“Petrological ( $P$ – $T$ ) mapping” of granulite–gneiss belts is beset with the problem of reconciling  $P$  and  $T$  estimates obtained using different geothermometers and geobarometers. It is especially acute in the most interesting and difficult cases, namely: (1) when the studied rocks have widely varying chemical and corresponding mineral compositions and (2) in the case of a thick crustal fragment with significant vertical variation of pressure and temperature. To solve this problem we have used a set of internally consistent individual temperature and pressure calibrations collected in the TPF program<sup>3</sup> (Fonarev et al., 1991,

<sup>3</sup> The TPF program may be obtained at the address [ftp.iem.ac.ru/pub/geology/tpf.zip](http://ftp.iem.ac.ru/pub/geology/tpf.zip) or on 3.5" IBM compatible diskette from the authors. The sensors included in the TPF system were additionally tested using experimental data (about 1500 experiments from 90 published studies), which were not available when TPF was originally developed. For testing, in addition to the experimental data, published analyses of minerals in natural assemblages, mostly containing appreciable additional components, were used as well. This test confirmed the high reliability and consistency of the Opx–Cpx, Grt–Opx, Grt–Cpx, and Grt–Crld geothermometers over wide compositional and  $P$ – $T$  ranges (e.g., Konilov et al., 1997; Mints and Konilov, 1998). Pressure estimates with the Grt–Opx–Pl–Qtz and Grt–Cpx–Pl–Qtz geobarometers are in good agreement with the data from recent experiments. For example, the average deviation of pressure estimates for the assemblage Grt–Opx–Cpx–Pl–Qtz is just 0.3 kbar (Konilov, 1999).

1994; Konilov, 1999). Maaskant (2004) has demonstrated good agreement between estimates obtained using those recommended by the TPF thermometers and barometers and the Thermocalc program.

As mentioned above, two generations of the gabbro–anorthosite bodies, 2.47–2.45 Ga and 2.1–1.91 Ga, are known in the lower part of the LGB succession (see Figs. 1 and 2). Their emplacements were followed by high-grade events, M0 and M1, which occurred closely after intrusion events at ~2.41 Ga and ~1.95 Ga. The M0 high-grade event in particular has been discovered in the Pyrshin gabbro–anorthosite massif in the LGB (see Fig. 2), however metamorphic conditions were not studied (Mitrofanov et al., 1995). Beyond the LGB, the earliest event (M0 according to our scale) was characterized by 990 °C at 12.4 kbar in the 2.45 Ga Kolvitsa massif (Fonarev and Konilov, 2005) and 700–900 °C at 10–12 kbar for small gabbro and diorite bodies in adjacent areas (Bogdanova, 1996).

Petrological observations evidence the multistage character of the metamorphic evolution of the LGB after emplacement of younger generation of gabbro–anorthosites (Hörmann et al., 1980; Mints et al., 1996; Perchuk et al., 1999). Mineral composition data on the granulite samples from several parts of the LGB published in the above listed papers were re-evaluated using thermometers and barometers from the TPF system.<sup>4</sup>

The pressure–temperature image of the LGB and footwall assemblages after emplacement of the younger generation of the gabbro–anorthosites is presented in Fig. 3. However, Fig. 3 is also a very important tool of the study. It provides important indications of:

- 1) The succession of metamorphic events: the first and more evident second ones are fixed mainly by  $P$ – $T$  parameters written in the compositions of the cores of mineral grains, the third one is written mainly in equilibrated compositions of touching homogeneous grains or their rims; the lower grade fourth event is written in the rim compositions of isolated grains; in some samples two or three successive mineral assemblages have been preserved, (Fig. 3, a and b);
- 2) The steep images of the M2, M3 and M4 successive paleogeotherms related to corresponding metamorphic events (Fig. 3, c);
- 3) The integrated character of the  $P$ – $T$ – $t$  array summarizing a number of individual  $P$ – $T$ – $t$  trajectories from various portions of the LGB (Fig. 3, d);
- 4) A concordant metamorphic evolution of the gabbro–anorthosite bodies localized at the base of the LGB and granulite–gneiss assemblage proper (Fig. 3, a–d).

<sup>4</sup> In particular, we have used experimentally based calibrations of the Opx–Cpx (Fonarev and Graphchikov, 1991), Grt–Opx (Perchuk and Lavrent'eva, 1990), Grt–Cpx (Powell, 1985), Grt–Bt (integrated from Holdaway and Lee, 1977; Perchuk and Lavrent'eva, 1983) and Grt–Crld (integrated from Thompson, 1976; Holdaway and Lee, 1977; Lavrent'eva and Perchuk, 1981; Ellis, 1986) geothermometers, which give values that do not deviate by more than 30 °C, and the Grt–Opx–Pl–Q (Graphchikov and Fonarev, 1990) and Grt–Cpx–Pl–Qtz (Fonarev et al., 1994) geobarometers, which differ by less than 1.5 kbar. The calibration of the Grt–Al<sub>2</sub>SiO<sub>5</sub>–Pl–Qtz geobarometer by Koziol and Newton (1989) was also used for metapelites.

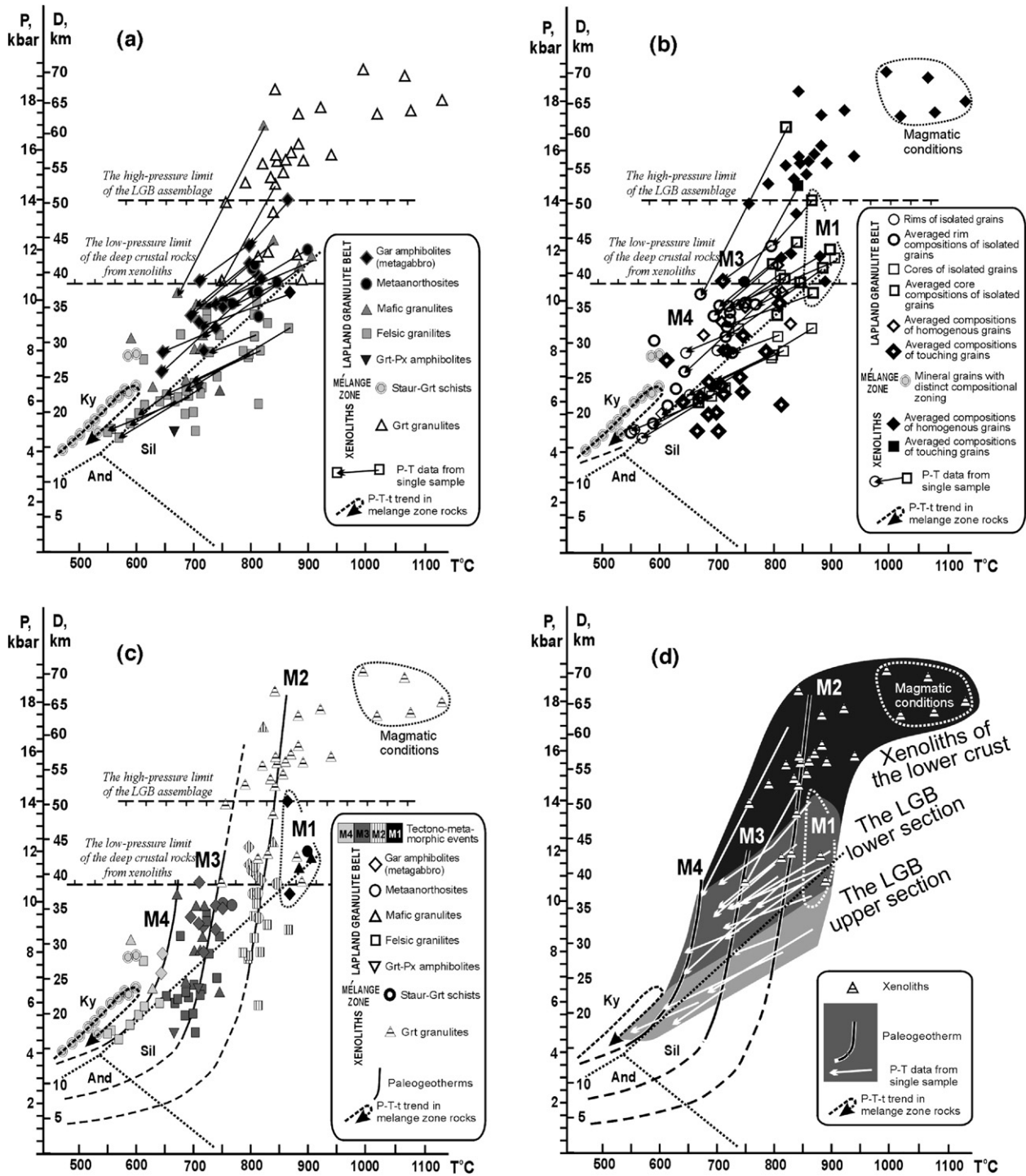


Fig. 3. *P*–*T* data for the Lapland granulite belt (based on recalculated data from Hörmann et al., 1980; Mints et al., 1996; Perchuk et al., 1999). Data on deep-seated crustal xenoliths were obtained on samples donated by V.R. Vetrin. *P*–*T* data from: a – various types of rocks, b – various types of mineral grains.

It is clearly seen also that during each stage the gabbro–anorthosites underwent metamorphism under higher pressures than the granulites proper, and thus must have lain at a deeper crustal level. The same relationships are indicated between the metagabbro–anorthosites and the garnet amphibolites (metagabbro). On the other hand, the *P*–*T* regularities displayed in Fig. 3 indicate the distinctly different metamorphic histories of metagabbro–anorthosites and garnet amphibolites *vis-à-vis* the

metasedimentary rocks within the mélangé zone (Tanaelv belt according to our understanding), which demonstrate a clockwise prograde–retrograde trend (see also Perchuk et al., 1999).

The petrological data indicate four stages in the evolution of the LGB (Fig. 3, c). The earliest event (M1: 960–860 °C, 14.0–10.3 kbar), restricted to the lowest part of the belt only, was practically coeval with emplacement of the younger generation of gabbro–anorthosite intrusions. The second event (M2) was

characterized by lower *P-T* conditions: from 860 °C at 12.4 kbar to 800 °C at 5.8 kbar, however one sample yielded a pressure estimate of 16.9 kbar. For the pervasive M3 metamorphism, the estimated *P-T* conditions were 770–640 °C at 10.7–4.8 kbar. Conditions for the final metamorphic stage, M4, were 650–550 °C at 8.4–4.5 kbar. Parameters of progressive metamorphism of the mélangé zone rocks at the base of the thrust nappe ensemble (the so called Korva Tundra gneisses and blastomylonites) show a clockwise *P-T* evolution that reached maximum values of 590–600 °C at ~8.5 kbar (Perchuk et al., 1999) (see Fig. 3). This documents rapid tectonic uplift and thrusting of the hot crustal slices during M4 resulting in inverted metamorphic zoning in the “parautochthonous” rocks and subsidence of tectonically thickened overloaded crust.

In Fig. 3 data from deep crustal xenoliths from Devonian pipes are also shown. A comparison of *P-T* values of granulite-facies metamorphism in xenoliths and in samples from the Lapland assemblage has demonstrated the co-ordination of the M2 “Lapland” geotherm with the geotherm from the xenoliths (see Fig. 3); the latter one extends the data from the LGB assemblage to deeper crustal levels.

### 3.2. Petrological mapping

The spatial distribution of *P-T* estimates for successive metamorphic events within the LGB area is shown in Fig. 4. It reveals a regular correlation between the *P-T* values and the sampling position. Samples with the highest *P* and *T* values are localized in the frontal part (at the southern boundary) of the thrust nappe belt. Northward, toward the back portion of the ensemble, *i.e.* the upper part of the LGB cross-section, *T* and *P*

become gradually lower. The samples with M1 *P-T* values belong to the lowest (frontal) portion of the belt only. Despite some deviations, the petrological maps (Fig. 4) suggest that mutual slipping during the tectonic displacement of the LGB crustal fragment was insignificant.

### 3.3. Seismic data and depth–temperature constraints

The deep structure of the LGB has previously been investigated along the Polar profile in the northern Finland (Marker et al., 1990) and in detail by vibroseismic reflection profiling along the Russia–Finland border (EGGI Profile) (Mints et al., 1996). The position of both profiles is shown in Fig. 2. Data from the seismic study along the EGGI profile together with geological mapping give a strong confirmation of the thrust structure of the LGB (Fig. 5). The present thickness of the LGB crustal slice as determined from reflection seismic data is around 18–20 km. Assuming 2.75 g/cm<sup>3</sup> as an average density of the crust, the thickness of the LGB crustal slice as characterized by metamorphic pressures for the M2 and M3 events reaching 21–23 km. It is clear that the thickness estimates obtained independently from the geological–geophysical and petrological data are in good agreement, considering the possibility of mutual sliding between single crustal sheets during thrusting. Cross-correlation of petrological and reflection seismic data permits us to interpret the metamorphic pressure values as real depth estimates: the M1 event is fixed in the lower part of the belt and occurred at 50–37 km depth. During the M2 event, the LGB assemblage was raised to depths of 44–21 km (these figures limit the lower and upper boundaries of the LGB crustal slice). Then, during M3, it

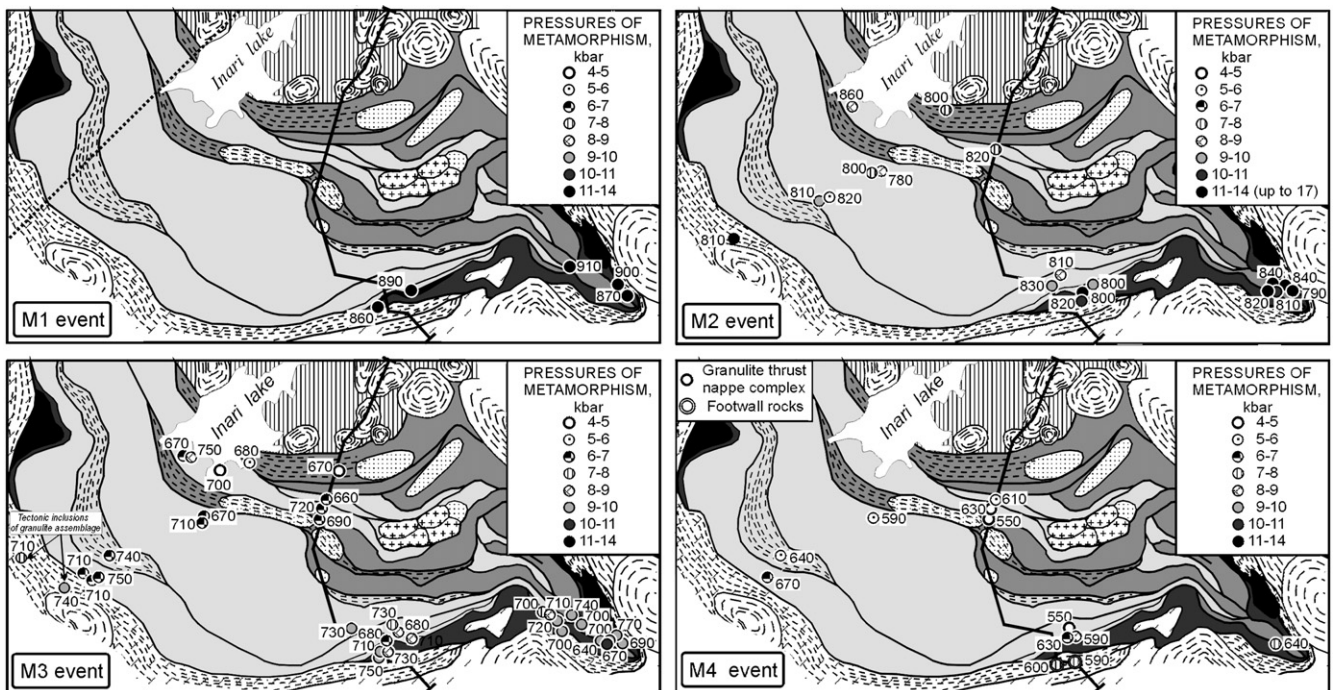


Fig. 4. Temporal, lateral and vertical variations of temperature and pressure of high-grade metamorphism in the Lapland granulite belt during the M1, M2, M3 and M4 metamorphic events. See Fig. 2 for legend.

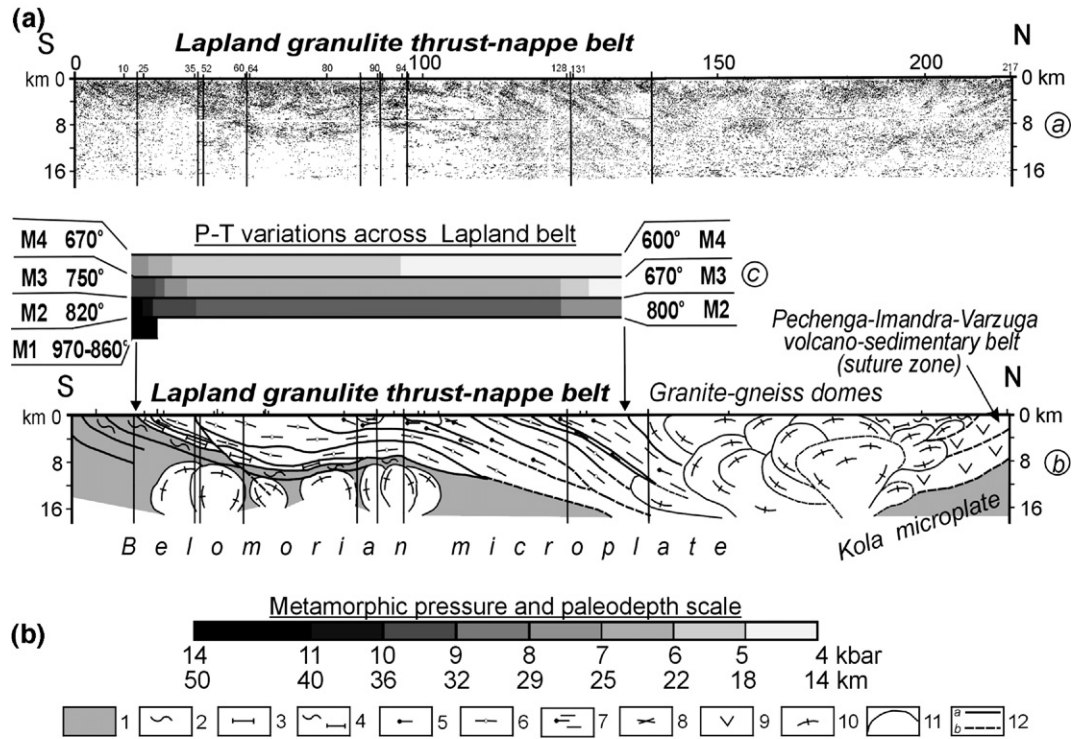


Fig. 5. Cross-section of the LGB: deep structure (reflection seismic data) and distribution of metamorphic pressures. Seismic data after Sharov (1997) and Mints et al. (1996), geological interpretation after Mints et al. (1996). 1: autochthonous complexes; 2: lower melange zone; 3–8: LGB— 3: metagabbro–anorthosites; 4: migmatized metagabbro–anorthosites; 5: mafic granulites; 6: khondolites; 7: Px-bearing diorites; 8: enderbites; 9: Pechenga volcano-sedimentary complex; 10: granite–gneiss domes; 11: geological boundaries; 12: main (a) and secondary (b) thrusts.

was raised to depths of 38–17 km and during M4 to 30–16 km depth. Mutual sliding of single layers and inclination of the crustal slice as a whole during overthrusting might perhaps explain the decrease of estimated thickness for the M4 event. Thus, the inferred thermal gradient within the lower crust during the granulite-facies metamorphism of the M2 and M3 events is 1.8–2.3 °C/km; during the M4 event it increased to 4–5 °C/km.

An integration of independent data sets along the POLAR profile (structural geology, refraction seismics, gravity, magnetics and electromagnetics) showed that the Tanaelv and the LGB form a thrust wedge, whose apex continues downward into the crust, where it is rooted at a depth of 15–20 km (Marker et al., 1990). Taking into account that the northeastern margin of the LGB is overturned exactly in the area crossed by the profile, a thickness of the LGB within the POLAR section can be estimated to be ~10–15 km. Petrological calculation based on data from the samples collected close to the POLAR profile yielded a thickness of ~12 km. As in the previous case, the petrological and geophysical estimates are in good agreement.

#### 4. Geochronology

##### 4.1. Initial magmatism (start of the Lapland granulite assemblage evolution)

Geochronological results testify to the long-term magmatic and tectono-metamorphic history of the LGB. The early

Palaeoproterozoic evolution of Laurentia at ~2.5 Ga started with the emplacement of mafic–ultramafic bodies (Mints and Konilov, 2004). Gabbro–anorthosite bodies were emplaced into the lower crust. The U–Pb dating of magmatic zircons and whole-rock Sm–Nd data reveal a 2.47–2.45 Ga intrusion age for gabbro–anorthosites in the eastern part of the LGB (Pyrshin and Kolvitsa massifs) (Mitrofanov et al., 1995; Frisch et al., 1995). Gabbro–anorthosites were followed by several injections of mafic dykes over the interval from 2.46 to 2.42 Ga. Every new batch of mafic dykes underwent extensional shearing and high-grade metamorphism during or immediately after solidification, and later dykes intruded into already sheared dykes (Balagansky et al., 2001). The earliest high-grade metamorphism has been dated 2.42–2.41 Ga by U–Pb ages of zircons in metamorphosed parts of the gabbro–anorthosite bodies (Mitrofanov et al., 1995). Layered peridotite–gabbro–norite intrusives were emplaced practically at the same time, 2.51–2.44 and up to 2.40 Ga, in the upper crust within a wide area of the eastern Fennoscandian Shield (Mitrofanov and Bayanova, 1999 and references therein).

##### 4.2. Second generation of the gabbro–anorthosite bodies

A second generation of layered gabbro–anorthosite intrusions was emplaced at the same deep crustal level as the first one simultaneously, or a little later, at the start of volcano-sedimentary processes considered below. An age for this event

has been estimated by the U–Pb zircon isochrons as 2.1–1.91 Ga (Bernard-Griffiths et al., 1984; Nerovich et al., 2004; Kaulina et al., 2004, 2005). In agreement with geochronological data, geochemical features also permit distinction of two anorthosite complexes. Anorthosites of the older generation have flat REE patterns with general contents characteristic for this type of rock ( $Ce_n=8.8–9.2$ ,  $Yb_n=2.15–3.73$ ,  $La/Yb_n=3.1–5.7$ ) with strong positive Eu anomaly ( $Eu/Eu^*=1.6–2.3$ ). For the majority of samples  $\epsilon_{Nd}$  has negative values (–0.3 to –2.1). This indicates an enriched mantle source or, more probably, crustal contamination of the mantle melts. Their crystallization was accompanied by primary fractionation and plagioclase separation. In the younger anorthosite generation the REE trend is characterized by more sharp inclination and lower HREE contents ( $Ce_n=8.9–12.4$ ,  $Yb_n=0.33–2.06$ ,  $La/Yb_n=6.7–48.9$ ) with a more significant positive Eu anomaly ( $Eu/Eu^*=2.8–4.7$ ) and  $La/Yb_n$  has positive correlation with  $Eu/Eu^*$ . Such REE patterns can be explained by significant garnet fractionation that suggests crystallization under high pressures (>18 kbar) and dry conditions and testifies to the greater depth of magma generation. For the majority of samples  $\epsilon_{Nd}$  has positive values: +1.2 to +3.65 that indicate a depleted mantle source for the younger anorthosites (Nerovich et al., 2004).

#### 4.3. Sedimentary protoliths

Protoliths of metasedimentary and meta-igneous granulites formed from approximately 2.1 to 1.91 Ga (Bibikova et al., 1993; Kaulina and Bogdanova, 1999; Daly et al., 2001; Glebovitsky et al., 2001; Kaulina et al., 2004; Glebovitsky, 2005). Sm–Nd whole rock and detrital zircon U–Pb ages show that metasediments contain both Palaeoproterozoic and Archaean detritus, with the former being markedly dominant (Bibikova et al., 1993; Bridgwater et al., 2001; Daly et al., 2001; Tuisku and Huhma, 2005). The U–Pb ages of 2.17 Ga (Kaulina and Bogdanova, 1999) and 2.14 Ga (Sorjonen-Ward et al., 1994) from multigrain detrital zircon fractions define the upper age limit of sedimentation. Some of the sediments could have been deposited at 1.95–1.93 Ga (Tuisku and Huhma, 2005). A few khondalite samples have yielded positive  $\epsilon_{Nd}(t)$  values varying from +0.1 to +1.1 at a Sm–Nd model age of 2.12 Ga (Daly et al., 2001) that indicate a juvenile nature for the source rocks. The lower age limit of sedimentation (and earliest deformation and metamorphism) of 1.94–1.91 Ga is provided by felsic and intermediate intrusions that cut the khondalites (Bibikova et al., 1993; Glebovitsky et al., 2001; Tuisku and Huhma, 2005). U–Pb zircon ages of 1.98 Ga for a garnet-bearing quartz diorite (Meriläinen, 1976) and of 2.06 Ga for a pegmatite vein in the Umba area (Kaulina and Bogdanova, 1999) suggest that some parts of the sedimentary protoliths were deposited and metamorphosed by those times.

#### 4.4. High-grade metamorphism

High-grade metamorphism in the LGB followed directly after emplacement of the younger generation of gabbro–anorthosites. According to Bernard-Griffiths et al. (1984), the

U–Pb, Rb–Sr and Sm–Nd data from the Vaskojoki anorthosite massif all yield coherent ages for this event within the range of 2.0–1.9 Ga. U–Pb zircon ages of 1.95–1.90 Ga for granulite-facies metamorphism of the Yaurijoki and Pyrshin anorthosites were obtained by Kaulina et al. (2004) and Nerovich et al. (2004). Bibikova et al. (1993) recognize two distinct metamorphic events: an earlier one at  $1925\pm 1$  Ma and a later one at  $1916\pm 1$  Ma. The existence of a younger stage of granulite-facies metamorphism was supported by 1912–1915 U–Pb zircon dates from the Kolvitsa zone (Balagansky et al., 2005). The ages of metamorphic zircons from leucosomes in migmatitic metasedimentary granulites, ages of rutile grains and Ar–Ar data all indicate that thrusting and related exhumation of the LGB assemblage occurred at about 1.88–1.87 Ga or later (Bibikova et al., 1993; Tuisku and Huhma, 2005; Daly et al., 2001; Balagansky et al., 2005).

### 5. New geochronological data

Though many geochronological investigations have been devoted to the LGB rocks, distinguishing the chronology of metamorphic stages has remained controversial. Recent U–Pb and Sm–Nd dating on minerals from metamorphic rocks of the area of the Yaurijoki and Pados rivers in the lower part of the LGB by T.Kaulina (Fig. 2, Tables 1–3) has permitted us to evaluate and discuss the temporal relationships between the younger gabbro–anorthosite generation, the succession of metamorphic events, and the cooling history of the LGB assemblage.

U–Pb and Sm–Nd analyses of accessory and rock-forming minerals were performed at the Laboratory for geochronology and isotope geochemistry of the Geological Institute of the Kola Science Centre of the Russian Academy of Sciences, Apatity, Russia.

Table 1  
Samples used for geochronological study (see Fig. 2 for location)

Sample code	Rock description
TAN-1	Amphibolite (metagabbro): $Grt_{58-62}+Cpx_{34-35}+Hbl_{46}+Pl_{52-53}$ . Garnet forms chemically unzoned grains. Local diaphthoresis.
Am-1	Amphibolite (metagabbro) – analogue of TAN 1
TAN-2	Plagiogneiss (metadiorite–leucogabbro): $Grt+Cpx+Hbl+Pl_{32}+Qtz$
TAN-3	Khondalite: $Sil+Grt_{56-61}+Bt_{34-36}+Pl_{36-37}+Qtz$
TAN-4	Leuco-to mesocratic mafic granulite: $Opx+Cpx+Bt^1+Pl+Qtz$ , strongly silicified. Secondary minerals: Qtz, blue-green Hbl, brown-green $Bt^2$ , carbonate and muscovite.
Ch-1	Leuco-to mesocratic mafic granulite: $Opx+Cpx+Bt^1+Pl+Qtz$
B-3694	Mafic granulite: $Cpx+Pl\pm Opx\pm Bt$ (5 m thick layer among fine-banded $Grt-Opx-Cpx$ and $Grt-Pl$ schists)
B-3693	Aplite-like granite: $Qtz+Pl\pm Fsp\pm Cpx\pm Bi^1$ . Granite intrudes $Grt$ amphibolite (metagabbro) having no traces of migmatization and deformation, thus fixing the upper age boundary of high-temperature structural-metamorphic transformations.
A-1, A-2, A-3	Anorthosites (Yavrozsky massif): $Cpx+Pl+Grt\pm Sph\pm Ru$ . Retrograde metamorphic assemblage: $Pl+Amp+Sc$ . Samples A-1 and A-3 – the least-altered anorthosite, sample A-2 – stripped anorthosite (for more details see Kaulina et al., 2004).
Am-2	Mafic dyke ( $Grt+Cpx+Opx$ ) cutting foliated anorthosites.

Table 2  
U–Pb isotopic data for zircons, titanites and rutiles from the investigated samples in the Pados–Yavr rivers area

No, mineral	Size, $\mu\text{m}$	Weight, mg	Concentration ppm		Pb isotopic composition			Isotopic ratio		Corr. coef.	Age, Ma
			Pb total	U	$^{206}\text{Pb}/^{204}\text{Pb}$	$^{206}\text{Pb}/^{207}\text{Pb}$	$^{206}\text{Pb}/^{208}\text{Pb}$	$^{207}\text{Pb}/^{235}\text{U}$ (%err)	$^{206}\text{Pb}/^{238}\text{U}$ (%err)		
<i>TAN-2 — garnet–clinopyroxene–amphibole plagiogneiss (metadiorite–leucogabbro)</i>											
1, Z	> 150	1.9	12.5	28	1984	8.2278	5.3023	5.4482 (1.30)	0.3365 (0.53)	0.55	1918 $\pm$ 20
TAN-2R	100–125	2.6	8.9	21	112	4.3047	2.7997	4.2394 (1.50)	0.2714 (0.58)	0.55	1853 $\pm$ 23
<i>TAN 3 — sillimanite–garnet–biotite gneiss (khondalite)</i>											
2, Z	100–150	3.6	33.9	74	1112	7.7635	2.3022	5.4237 (0.37)	0.3360 (0.25)	0.73	1912 $\pm$ 5
TAN-3R	> 100		9.1	23	259	6.0480	6.3530	5.2798	0.3351		1869 $\pm$ 21
<i>TAN-4 — biotite–two-pyroxene plagioclase schist (mafic granulite)</i>											
3, Z	150–200	5.2	27.5	70	2857	8.2142	5.1995	5.5912 (0.29)	0.3456 (0.19)	0.71	1916 $\pm$ 4
4, Z	150–200	6.7	27.9	65	462	6.8540	3.9532	5.5570 (0.35)	0.3437 (0.23)	0.71	1915 $\pm$ 5
5, Z	150–200	4.2	22.5	56	1735	8.0240	4.5380	5.5934 (0.36)	0.3461 (0.17)	0.64	1914 $\pm$ 5
TAN-4R	150–200	2.4	12.3	44	649	7.3897	15.6087	4.2989 (1.10)	0.2712 (0.82)	0.79	1880 $\pm$ 12
<i>Ch-1 amphibole–two pyroxene plagioclase schist (mafic granulite)</i>											
6, Z	150–250	4.8	13.4	35	976	7.6570	5.3949	5.4794 (0.57)	0.3390 (0.26)	0.59	1914 $\pm$ 8
<i>B-3694 — two-pyroxene–plagioclase schist (mafic granulite)</i>											
7, Z	250–300	2.2	110.7	269	9514	8.4534	3.4836	5.4988 (0.50)	0.3404 (0.50)	0.95	1913 $\pm$ 2
8, Z	200–250	2.5	113.3	270	3770	8.3004	3.5964	5.6161 (0.50)	0.3476 (0.50)	0.95	1914 $\pm$ 2
9, Z	250–300	2.2	133.8	313	2969	8.2121	3.4963	5.5843 (0.50)	0.3451 (0.50)	0.90	1917 $\pm$ 2
<i>B-3693 — aplite-like granite</i>											
1, Z	<200	1.9	139.3	383	2796	8.2322	9.4415	5.5523 (0.64)	0.3447 (0.63)	0.99	1908 $\pm$ 2
2, Z	<200	2.3	123.8	354	6241	8.4187	10.2115	5.3860 (0.50)	0.3345 (0.50)	0.94	1908 $\pm$ 2
3, Z	<150	2.2	117.8	341	8140	8.4939	11.4280	5.3426 (0.70)	0.3331 (0.70)	0.83	1901 $\pm$ 3
4, Z	<150	1.1	176.7	520	666	7.3045	7.6758	4.9223 (0.70)	0.3049 (0.70)	0.75	1912 $\pm$ 4
T	>125	1.3	82.1	117	81.4	3.5631	1.1936	5.0273 (4.80)	0.3127 (4.80)	0.99	1905 $\pm$ 10
<i>TAN-1 — garnet–clinopyroxene amphibolite (metagabbro)</i>											
TAN-1R	>160	5.1	8.8	7	38	2.1270	0.7477	5.2350 (3.80)	0.3296 (0.62)	0.71	1883 $\pm$ 60
TAN-1T <sub>1</sub>	160–200	5.2	21.6	17	42	2.2900	0.6797	4.9022 (3.90)	0.3128 (0.63)	0.46	1859 $\pm$ 65
TAN-1T <sub>2</sub>	160–200	2.6	7.6	10	78	3.4800	0.6847	4.3250 (3.50)	0.2716 (0.72)	0.54	1888 $\pm$ 57
<i>A-1, A-2, A-3 — anorthosite</i>											
A-3 T		1.7	8.9	19	100	4.0449	1.0101	4.8853 (2.00)	0.3102 (0.80)	0.65	1868 $\pm$ 21
A-1 R*		4.8	2.00	9	939	7.7565	19.2001	3.6721 (2.00)	0.2321 (2.00)	0.99	1876 $\pm$ 3
A-2 R <sub>1</sub>		5.35	16.79	27	71	3.3191	2.835	5.1478 (1.50)	0.3261 (1.50)	0.90	1872 $\pm$ 12
A-2 R <sub>2</sub>		1.9	10.87	25	170	5.2029	4.629	5.1606 (1.50)	0.3292 (1.50)	0.42	1859 $\pm$ 29
<i>Am-1 — garnet–clinopyroxene amphibolite (metagabbro)</i>											
Am-1 R		0.75	6.05	21	48	2.5549	1.2704	4.4816 (1.50)	0.2846 (1.20)	0.55	1867 $\pm$ 23
<i>Am-2 — garnet–pyroxene dyke</i>											
Am-2 R		1.8	5.95	23	129	4.4434	3.2859	3.8805 (1.51)	0.2453 (0.69)	0.62	1876 $\pm$ 22

Pb and U were measured by the isotopic dilution technique with a mixed  $^{208}\text{Pb}$ – $^{235}\text{U}$  tracer on Finnigan-MAT 262 (multi-collector) and MI-1201T (single collector) mass spectrometers. Pb isotope ratios were corrected for mass fractionation with a factor of 0.10% per amu (Finnigan MAT-262) and 0.18% per amu (MI-1201T). Total procedural blanks were 0.1–0.3 ng for Pb and 0.05 ng for U. The U analyses were corrected for mass fractionation with a factor of 0.003% per amu (Finnigan MAT-262) and 0.08% per amu (MI-1201T). The U decay constants were taken from Steiger and Jäger (1976). The correction due to non-radiogenic lead impurity was done using the model of Stacey and Kramers (1975). All calculations were done using the programs PBDAT and ISOPLOT (Ludwig, 1991, 1999).

\*This sample was measured on the Finnigan-MAT 261 in the Swedish Museum of Natural History, Stockholm Z – zircon, T – titanite, R – rutile.

### 5.1. Zircon ages

Zircons from khondalite (TAN-3), mafic granulites (TAN-4, B-3694 and Ch-1) and Grt–Cpx amphibolites (metagabbro) (TAN-1, Am-1 and TAN-2) (Table 1) have been studied. The metamorphic zircons in the samples of granulite-facies rocks are crystals of similar image (Fig. 6a). They are round or isometric

large crystals with bright luster and high transparency, colorless or weakly yellowish-pink. Zircons are characterized by low U contents (up to 100 ppm) and high Th/U and Zr/Hf ratios (0.6–0.7 and 42–49, respectively) typical for zircons formed under high  $\text{D}\text{O}$ -parameters (Bibikova et al., 1993). All results are concordant or slightly discordant, yielding  $^{207}\text{Pb}/^{206}\text{Pb}$  ages of 1918–1912 Ma (Table 2). The upper intersect age of zircons in

Table 3  
Sm–Nd data for the studied rocks and minerals

Samples	Concentration ppm		Isotopic ratios	
	Sm	Nd	$^{147}\text{Sm}/^{144}\text{Nd}$	$^{143}\text{Nd}/^{144}\text{Nd}$
<i>TAN-1— garnet–clinopyroxene amphibolite (metagabbro)</i>				
WR	1.338	4.095	0.19750	0.512740
Grt	1.23	1.11	0.66822	0.518532
<i>TAN-2 — garnet–clinopyroxene–amphibole plagiogneiss (metadiorite–leucogabbro)</i>				
WR	4.49	18.9	0.14319	0.511983±12
Cpx	11.99	51.9	0.14184	0.511959±9
Ap	192.80	1343.0	0.08676	0.511299±11
Grt	6.95	6.36	0.65986	0.518514±6
Pl	0.39	2.32	0.10239	0.510938±8
<i>TAN-3 — sillimanite–garnet–biotite gneiss (khondalite)</i>				
WR	6.10	30.8	0.11971	0.511474±5
Bt	3.47	16.6	0.12640	0.511586±6
Grt	10.5	8.2	0.76929	0.519578±7
Mi	1.90	22.3	0.05147	0.510645±9
Ap	2.94	17.1	0.10392	0.511421±20

Isotopic ratios were measured on Finnigan MAT-262 mass-spectrometer.  $^{143}\text{Nd}/^{144}\text{Nd}$  ratios were normalized to  $^{146}\text{Nd}/^{144}\text{Nd}=0.7219$ . During the course of this work, the mean value for the  $^{143}\text{Nd}/^{144}\text{Nd}$  obtained for the La Jolla standard was  $0.511833\pm 6$  ( $2\sigma$ ,  $n=11$ ). A minimum error of 0.003% was chosen based on the reproducibility of the La Jolla standard. Nd blanks were less than 0.3 ng, and Sm blanks were less than 0.06 ng.

five studied samples (nine fractions) is  $1915\pm 2$  Ma (Fig. 6a). The aplite-like granite (B-3693) contains light-brown short prismatic, mainly flattened high-U (341–520 ppm) zircon crystals (Fig. 6b). Four fractions define a discordia line with an upper intercept of  $1905\pm 14$  Ma.

### 5.2. Titanite and rutile ages

Besides zircons, practically all samples contain rutile and titanite (Table 2, Fig. 6c). Anorthosites of the Yavrosersky massif contain two types of titanites: dark-brown large grains of irregular shape and light yellow transparent rounded slightly flattened crystals. The U–Pb age of brown titanite is  $1916\pm 12$  Ma (Kaulina et al., 2004). Light titanite has a  $^{207}\text{Pb}/^{206}\text{Pb}$  age of  $1868\pm 21$  Ma (Table 2, Fig. 6c). Similar light titanite occurs in the Grt–Cpx amphibolite (metagabbro TAN-1). Two fractions yielded similar  $^{207}\text{Pb}/^{206}\text{Pb}$  ages:  $1859\pm 65$  and  $1888\pm 57$  (Table 2). The large uncertainty in the  $^{207}\text{Pb}/^{206}\text{Pb}$  ages was caused by very low U contents in light titanite. Brown titanite from an aplite-like granite sample represented by large (up to 250  $\mu\text{m}$ ) grains and their fragments yielded a  $^{207}\text{Pb}/^{206}\text{Pb}$  age of  $1905\pm 10$  Ma, which coincides with the zircon age of the rock. All rutile grains from the studied samples (TAN-1, TAN-2, TAN-3, TAN-4, Am-1, Am-2, A-1, A-2) have ages within the limits of 1.86–1.89 Ga (Table 2, Fig. 6c) similar to the age of light titanite.

### 5.3. Sm–Nd ages

Grt–Cpx amphibolite (metagabbro TAN-1), Grt–Cpx–Hbl gneiss (metaleucogabbro TAN-2) and Sil–Grt–Bt gneiss

(khondalite TAN-3) are characterized by whole rock–mineral isochrons of various ages (Table 3, Fig. 6d–f) and reflect different processes. The isochron for Grt+Cpx+WR of sample TAN-2 defines an age of  $1922\pm 9$  Ma (Fig. 6d). The isochron for Grt+Cpx+WR+Ap (TAN-2) defines an age of  $1918\pm 30$  Ma with large MSWD=5.4. The isochron calculated for Mi+Bt+Grt+WR of sample TAN-3 defines an age of  $1892\pm 21$  Ma (Fig. 6e). Garnet from sample TAN-1 yielded a Sm–Nd age (Grt+WR) of  $1870\pm 11$  Ma (Fig. 6f). The same age (Grt+WR) was obtained for garnet from migmatite of the LGB ( $1870\pm 7$  Ma, Daly et al., 2001).

## 6. Discussion

### 6.1. Petrological speculations

The prominent feature of the thermal structure of the exhumed LGB crustal section is a very low geothermal gradient within the lower crust during M2, M3 and M4 events; the causes of which remain unclear so far. High thermal conductivity during granulite-facies metamorphism could be explained by pervasive fluid flow and intense deformation, temperature stabilization across the extensive crustal section due to partial melting could be of significance too. Heat transfer due to ascending partial melts may also play a role. In any case, it seems clear that the lower crust under granulite-facies conditions appears have to be a very effective heat conductor. On the other hand, high levels of heating of the crust require rapid input of a large amount of mantle-derived heat. In this regard, the model of Palaeoproterozoic superplume events in the eastern Fennoscandian Shield at  $\sim 2.5$  Ga and  $\sim 2.0$  Ga postulated by many researchers (see Mints and Konilov, 2004 and references therein) is highly attractive.

The actual scale and significance of the M0 and M1 events remain obscure, as there are no unambiguous data on the possible age of mafic granulites in the lower part of the LGB. Balagansky et al. (2001) suggest, on the basis of geological relationships, that emplacement of the protoliths of the mafic granulites of the Kolvitsa and Por'ya Guba units must have been broadly coeval with gabbro–anorthosite intrusion at  $\sim 2.45$ –2.4 Ga. Additional confirmation comes from the study of xenoliths of Palaeoproterozoic lower crust hosted by Devonian pipes (Kempton et al., 2001). These xenoliths are predominantly garnet granulites, which resemble in composition the mafic granulites of the LGB. The geochemical features of the xenoliths indicate their provenance from underplating of mantle-derived magmas. Grt and Cpx in the xenoliths occur in roughly equal amounts, but Fsp (Pl and a minor K-feldspar) ranges from  $\sim 85\%$  to less than 5% by volume. As a result these rocks range in bulk composition from norite and gabbro–norite to gabbro–anorthosite (Kempton et al., 1995; Vetrin, 1998). The age of the earliest granulite-facies metamorphism in the lower crust of the LGB is poorly constrained. Plagioclase–whole rock Pb–Pb data suggest two main metamorphic events during the Palaeoproterozoic at  $\sim 2.4$  Ga and  $\sim 1.8$  Ga (Neymark et al., 1993). Besides, an age of the earliest garnet crystallization in the granulite xenoliths has been estimated by Pb–Pb isochron as

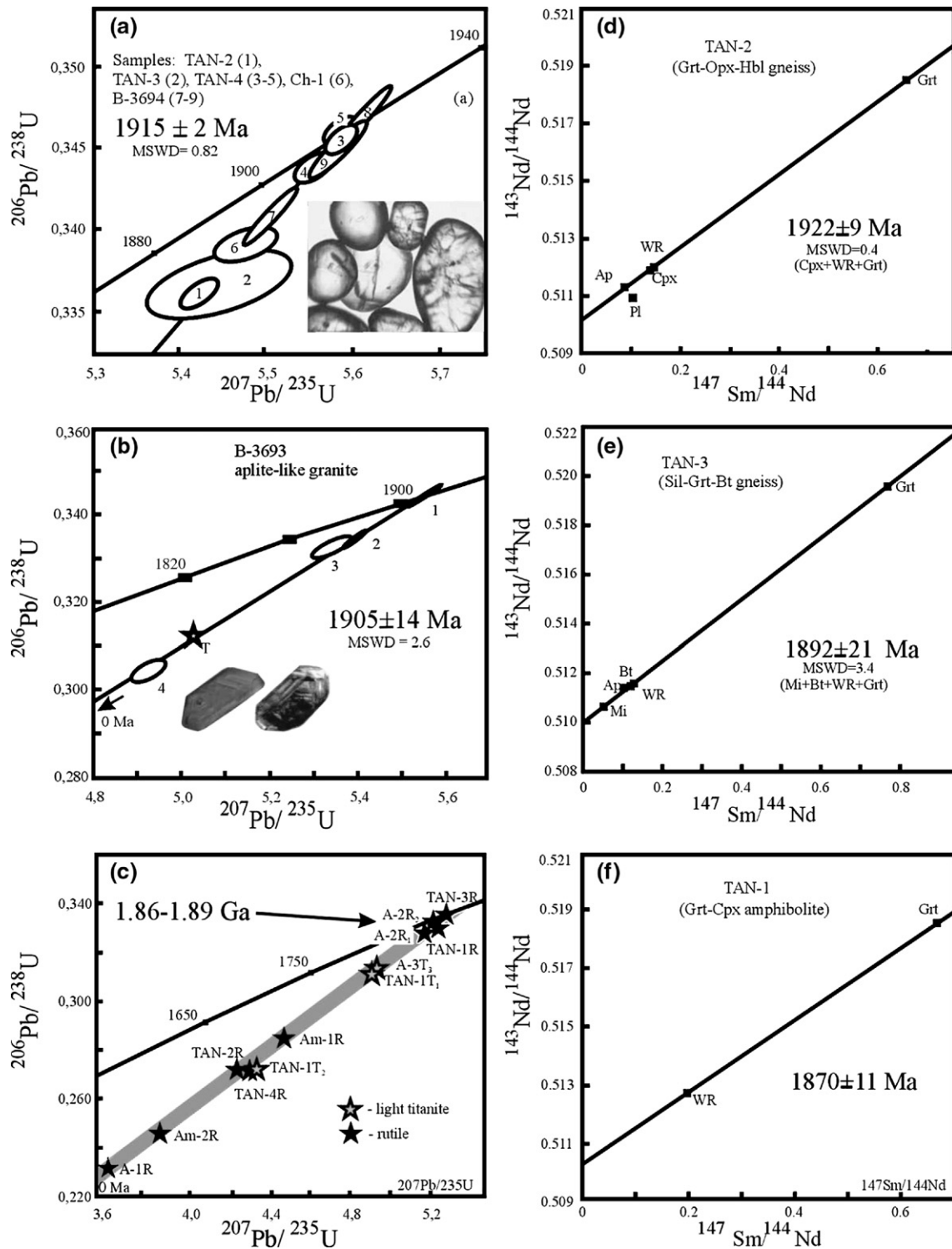


Fig. 6. Results of geochronological study. a–c — U–Pb concordia diagrams: a – zircons from khondalite (TAN-3), mafic granulites (TAN-4, B-3694 and Ch-1) and Grt–Cpx–Hbl gneiss (TAN-2), inset – typical image of zircons from the granulite-facies rocks in the LGB, transmitted light; b – zircons from aplite-like granite; c – rutiles and titanites; d–f — Sm–Nd isochrons: d – Grt–Cpx–Hbl gneiss, e – Sil–Grt–Bt gneiss, f – Grt–Cpx amphibolite.

$2.56 \pm 0.41$  Ga; the concordant U–Pb age of garnet in one of the analyzed samples is 2.59 Ga (Kempton et al., 2001).

On the other hand, comparison of  $P$ – $T$  values of granulite-facies metamorphism in xenoliths and in samples from the Lapland assemblage has demonstrated the co-ordination of the

M2 “Lapland” geotherm with the geotherm from the xenoliths (see Fig. 3). It is important to note that the latter one extends the data from the LGB assemblage to deeper crustal levels. It is clear from Fig. 3 that the thermal evolution of the LGB cannot be presented in routine  $P$ – $T$ – $t$  terms. No single  $P$ – $T$ – $t$  trajectory can

be considered as characteristic for a process in general. Inverted metamorphic zoning in the footwall rocks is a consequence of heating from the overthrust hot slices of the LGB proper.

### 6.2. Interpretation of geochronological data

Comparison of above listed time intervals related to magmatic, metamorphic and sedimentation events suggests a coincidence of ages of not only the younger generation of the gabbro–anorthosite intrusions (2.1–1.95 Ga) and high-grade metamorphic events (2.0–1.9 Ga), but also their tight similarity with timing of sedimentation (from 2.2 to 1.94–1.91 Ga). Approximately 1.92–1.91 Ga ago, following emplacement of 2.1–1.95 Ga gabbro–anorthosites, metamorphic crystallization of zircon took place in a wide range of LGB assemblages. As morphology, isotopic composition and trace element contents are similar, it occurred most probably under the same conditions. Zircon ages obtained are to be related not to the *P–T* peak but to start of decompression and cooling, which followed soon after the peak (Watson and Harrison, 1983; Roberts and Finger, 1997). Results of Sm–Nd dating lead us to the same conclusion. The Sm–Nd age of the Grt–Cpx–Hbl gneiss is  $1922 \pm 9$  Ma. As the closure temperatures (*T<sub>c</sub>*) for the Sm–Nd system in the used minerals are different,  $\sim 650$  °C in Grt (Mezger et al., 1991) and about 800 °C in Cpx (Sneeringer et al., 1984), this rock probably cooled quickly from 800 to  $\sim 650$  °C and resulted in almost simultaneous closure of related isotopic systems. Perchuk et al. (1999) showed: (1) clinopyroxene was growing due to decreasing pressure, as cores of clinopyroxene grains contain up to 10% of the jadeite end-member, whereas the rims contain only about 2%; (2) isobaric cooling with decrease of temperature from 725 °C to 657 °C took place just after the decompression. The  $1916 \pm 12$  Ma age of titanite from anorthosite of the Yavrozsky massif (Kaulina et al., 2004) confirms a decrease in temperature at this time at least to 700 °C (*T<sub>c</sub>* for titanite U–Pb system, Cherniak, 1993).

The M1 late-magmatic (autometamorphic) event must have occurred around 1.95 Ga. It is seen from interrelation of the petrological and geochronological data that the peak metamorphism M2 (830–800 °C) occurred before 1.92 Ga and the M3 event (750–700 °C) was completed by approximately 1.92–1.90 Ga. The aplite-like granite (that does not contain magmatic hydroxyl-bearing minerals) was formed under conditions close to, or slightly, below granulite facies.

Hence, the  $1905 \pm 14$  Ma age of magmatic zircons from this rock provides an upper time limit for the transition from granulite to amphibolite facies, when temperatures decreased below 650–600 °C. At the same time, 1.91–1.90 Ga, high-*U* metamorphic zircons were formed everywhere in the LGB assemblages (Mitrofanov et al., 1995; Frisch et al., 1995; Kaulina et al., 2004). A somewhat younger stage of metamorphic evolution is fixed by Sm–Nd mineral ages from Sil–Grt–Bi gneiss (khondalite). As mentioned above, *T<sub>c</sub>* for the Sm–Nd system in garnet is  $\sim 650$  °C. Accepting that *T<sub>c</sub>* for microcline is close to that in plagioclase, 560–600 °C (Ganguly and Turone, 2001), and for biotite is slightly lower, one may conclude that temperature became near to, or lower than 600 °C

by 1.89–1.87 Ga. This temperature corresponds to the M4 event related to collisional thickening of the crust. Similar U–Pb dates were obtained from rutile and titanite grains. The *T<sub>c</sub>* for lead diffusion in rutile is *ca.* 450 °C; hence, we conclude that further cooling occurred rapidly. Light titanite grains have the same U–Pb ages (1.89–1.86 Ga). As *T<sub>c</sub>* for the U–Pb system in titanite is around 700 °C (Cherniak, 1993), this age is interrelated to the timing of low-temperature growth of this mineral.

Thus, the high-grade metamorphism in the LGB lasted from 1.95 to 1.91–1.90 Ga. Collision crustal thickening, latest deformation and retrograde reactions took place at 1.89 to 1.87 Ga.

### 6.3. Geodynamic evolution

The main constituents of the Kola–Karelian Palaeoproterozoic orogen are fragments of the former Neoproterozoic continent (Murmansk, Central-Kola, Belomorian, Karelian and some others) separated by a network of Palaeoproterozoic low-grade volcano-sedimentary belts (see Fig. 1), at least some of which have been interpreted as sutures (Mints and Konilov, 2004 and references therein). Like the low-grade volcano-sedimentary belts, the LGB is a juvenile Palaeoproterozoic crustal unit situated within the Kola–Karelia orogen. Its major distinction lies in the high-grade metamorphism of the rocks. In fact, the LGB is situated between three sutures (Pechenga–Imandra–Varzuga, Karasjok and North-Karelian belts) plunging towards each other. Hence, the depositional basin corresponding to the LGB (“back-arc basin”) could be related to any of them. Besides, the almost contemporaneous global-scale occurrences of crustal extension events (Mints and Konilov, 2004 and references therein), which in some cases have no relationship to any kind of subduction, suggest the independent nature of both processes: an extension within the area of the Lapland sedimentary basin and subduction in adjacent Palaeoproterozoic oceans.

Conclusions obtained from combined geodynamic interpretation of the above data depend crucially on understanding of the position of the gabbro–anorthosite bodies involved in the evolution of the LGB. The above-described situation with two generations of gabbro–anorthosite intrusions is not unique. It is well known that large layered gabbro–anorthosite bodies of two or more generations are included in many granulite belts worldwide (e.g., Grenville Province, Dzhugdzhur–Stanovoy belt, Sveco–Norwegian belt). The close interrelations between granulite-facies rocks and gabbro–anorthosites cannot be coincidental. It has been suggested that emplacement of massif type anorthosite plutons in the Grenville Province followed directly on from major crustal thickening events, and occurred during crustal extension in convergent orogens (Martignole, 1996). An important feature of the LGB is the localization of both generations of gabbro–anorthosite bodies within a narrow zone at the base of the granulite belt. This peculiarity might be explained by consecutive under- and interleaving of mantle-derived mafic magmas within the lower crust. Later, crustal delamination and collision-related crustal shortening resulted in tectonic emplacement of fragments of deep-seated gabbro–

anorthosite bodies of both generations at the base of the thrust nappe ensemble.

The inferred scheme of geodynamic and metamorphic evolution of the LGB and adjacent structures based on a combined plume–plate tectonics model (Mints and Konilov, 2004) is shown in Fig. 7. An emplacement of the first generation of gabbro–anorthosite and the M0 stage of granulite-facies metamorphism were broadly coeval with initial Palaeoproterozoic, plume-influenced rifting of a Neoproterozoic supercontinent at 2.51–2.44 (2.40) Ga. This period was followed by the deposition of volcano-clastic protoliths of the LGB assemblage, which is inferred to have occurred within an intracratonic depression or in a back-arc extensional basin at 2.44–2.11 (2.0) Ga. The new plume-related extension that induced emplacement of the second generation of gabbro–anorthosite bodies, lasted from 2.11 (2.0) to 1.95 Ga. The M1 high-grade

metamorphism and then the pervasive M2 granulite-facies metamorphism followed at about the end of this period. Data from the low-grade volcano-sedimentary belts during the same period indicate opening and subsequent closure of the intracontinental oceans due to rapid subduction and/or obduction of oceanic lithosphere (Melezhik and Sturt, 1994; Mints et al., 1996; Peltonen et al., 1998). The overlapping of ages of gabbro–anorthosite intrusions (2.1–1.95 Ga) and subduction processes in the Pechenga–Imandra–Varzuga belt (~1.96 Ga) causes uncertainties in the nature of delimitation between extensional and compressional stages. This temporal overlapping may be a real feature of crustal evolution; in particular, it may be a consequence of interaction of plume and plate tectonic related processes. A number of data provide evidence for an astonishingly rapid crustal evolution during the 1.95–1.89 Ga interval. This comprised: (1) emplacement of mantle-derived

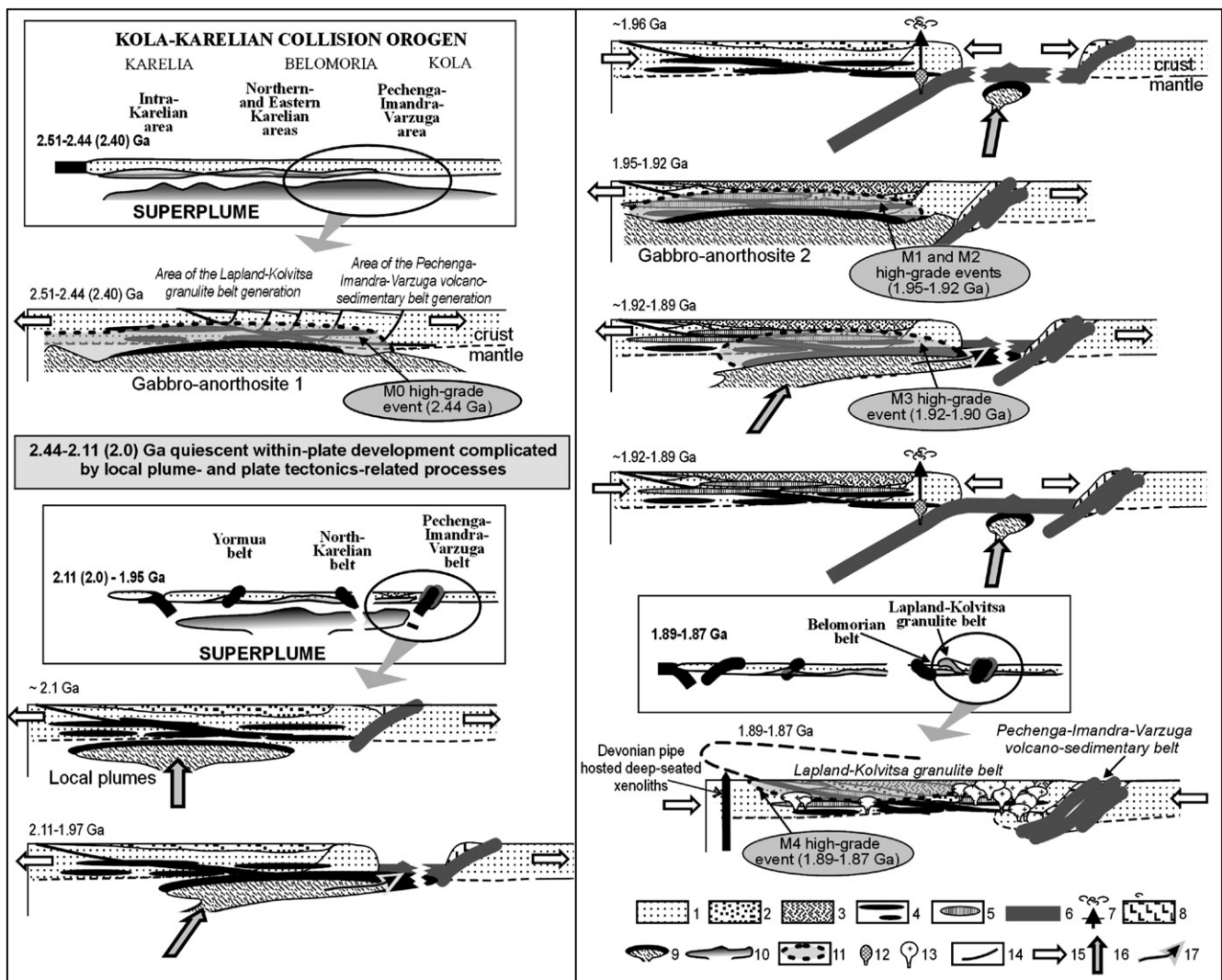


Fig. 7. Geodynamic evolution of the LGB. 1: the Archaean lithosphere (crust–mantle boundary is marked); 2–17: Palaeoproterozoic assemblages and processes— 2–3: volcano-sedimentary sequences deposited in rift (2) and in back-arc ensialic basins (3); 4–5: layered mafic bodies, mostly gabbro–anorthositic, emplaced 2.47–2.43 Ga (4) and 1.95 Ga (5) ago; 6: oceanic-type crust; 7–8: suprasubduction features—volcanic activity (7); sedimentary–volcanic assemblages (8); 9–10: mantle plumes (hot mantle upwelling)— 9: at the LGB cross-section; 10: at the regional cross-section; 11: high-grade metamorphic aureoles; 12: suprasubduction magma chambers; 13: granite–gneiss domes; 14: faults; 15: tectonic strain; 16: hot mantle movements; 17: heat discharge in the direction of maximum thermal gradient.

mafic magmas in the lower crust at  $\sim 1.95$  Ga; (2) creation of an extended sedimentary basin in which a more than 10 km-thick (see Fig. 7) volcano-sedimentary succession of the future LGB was deposited during a short period from  $\sim 1.95$  to  $1.91$  Ga; (3) pervasive granulite-facies metamorphism of the rocks within crustal section from  $\sim 70$  to  $\sim 25$  km depth (see Fig. 3). Correlation of geochronological and petrological data permit us to distinguish two granulite-facies metamorphic events: M2 between  $1.95$  and  $1.92$  Ga and M3 at approximately  $1.92$ – $1.90$  Ga. The M1, M2 and M3 events were probably initiated by a superplume beneath the Kola–Karelian region: its main pulse started at  $\sim 2.1$ – $2.0$  Ga with the maximum activity at  $1.95$  Ga. As there is no evidence for subduction of the LGB volcano-sedimentary deposits during this short interval, and especially due to the common metamorphic history of this assemblage and extension-related gabbro–anorthosite intrusions, we conclude that the granulite-facies metamorphism of the sediments was the result of an expanding high-grade metamorphic aureole into the lower part of the sedimentary succession.

However, how could the sediments have been deposited directly onto lower crustal assemblages? We see the probable explanation in the rapid development of the deep sedimentary basins and granulite-facies metamorphism at the lower- and mid-crustal levels above a mantle plume. Significant crustal stretching may, under certain conditions, result in the gradual removal of the upper crustal blocks and direct contact of mid- or even deep-crustal rocks with sediments rapidly being deposited in the subsiding basin. An example of a deep crustal extensional shear zone developed at  $\sim 2.44$  Ga simultaneously with injections of mantle derived mafic magmas has been well described by Balagansky et al. (2001) for the Kolvitsa unit of the LGB. Coincidence of orientation of multiple dykes, foliation and primary magmatic layering in the gabbro–anorthosites indicate that the shear zone must have been initially subhorizontal. As Harris et al. (2002) have shown experimentally, many of fold geometries usually attributed to convergent tectonic settings may develop in an extensional environment.

Cessation of metamorphism was possibly triggered by a transition from an initial extension to spreading at the flanks of a rift basin, *i.e.* within the area of the Pechenga–Imandra–Varzuga and other volcano-sedimentary belts (see Fig. 7). Only the M4 event has to be related to collision thickening of the crust at  $1.89$ – $1.87$  Ga and this coincided with accretion of the Svecofennian island arcs. Stacking of crustal slices during final Palaeoproterozoic collision resulted in formation of the LGB thrust nappe ensemble. The Palaeoproterozoic evolution in the eastern Fennoscandian Shield was terminated at approximately  $1.77$  Ga with the general collision of the fragments of the former Neoarchaean supercontinent and juvenile Palaeoproterozoic terranes, doming within thickened crust, and an orogenic magmatism (Gaál and Gorbatshev, 1987; Mints et al., 1996).

## 7. Conclusion

A combined plume–plate tectonics model of geodynamic and metamorphic evolution of the LGB and adjacent structures

integrates the available geological, petrological, geochronological and seismic reflection data. The main lines of the metamorphic evolution of the LGB are as follows.

1. The main high-grade metamorphic events are interpreted to reflect the plume-related extension stages at  $\sim 2.44$  (M0) and at  $\sim 2.0$ – $1.95$  Ga (M1). Subsequent events at  $\sim 1.95$ – $1.92$  Ga (M2) and  $\sim 1.92$ – $1.90$  Ga (M3) were possibly coupled with extensional settings also. Cessation of metamorphism was triggered by transition from an initial rift stage to spreading at the flanks of the rift basin.
2. Only the last (M4) event at  $\sim 1.89$ – $1.87$  Ga corresponds to the final collision stage. It was linked with deformation processes and crustal stacking. The inverted metamorphic zoning in the autochthonous rocks was a consequence of heating beneath hot overthrust slices of the LGB proper.
3. Temperatures and pressures of high-grade metamorphism within the LGB assemblage during the M1 event ranged from  $960$  to  $860$  °C and from  $14.0$  to  $10.3$  kbar; during the M2 event they decreased from the lower to upper part of the LGB assemblage from  $860$  °C at  $12.4$  kbar to  $800$  °C at  $5.8$  kbar; during the M3 event from  $770$  °C at  $10.7$  kbar to  $640$  °C at  $4.8$  kbar, and during M4 event from  $650$  °C at  $8.4$  kbar to  $550$ – $500$  °C at  $4.5$  kbar.
4. The thermal gradient within the lower crust during the granulite-facies M2 and M3 metamorphic events was  $1.8$ – $2.3$  °C/km, and during the M4 event it reached  $4$ – $5$  °C/km.
5. The agreement of thickness estimates of the granulite ensemble obtained from seismic data with those calculated from petrological barometry attests to the lithostatic nature of metamorphic pressure. According to both estimates the average thickness of the Lapland granulite slice was initially  $\sim 21$ – $23$  km.

It is important to note that the characteristic feature of the thermal structure of the crust during high-grade metamorphism, which have been inferred in the LGB, were recorded in a number of granulite belts of various ages worldwide (Mints and Konilov, 1998 and references therein).

## Acknowledgements

This work has been supported by the Russian Foundation for Basic Research (01-05-64373, 04-05-64059 and 05-05-65012 and by Scientific school SC-1413.2006.5). The authors thank V.I. Fonarev, V.P. Andreev, L.I. Nerovich and E.Ya. Shenkman for the donation of the granulite samples and V.R. Vetrin for the permission to study his samples of deep-seated crustal xenoliths and for the useful discussion. The main conclusions of this paper are the direct result of fruitful work and discussions with V.V. Balagansky, M. Marker, J.S. Daly, H. Downes and other colleagues at workshops managed in the context of SVEKALAPKO (Europrobe project). The first version of this paper was significantly reworked as a result of the helpful comments of Prof. M. Raith, Prof. S. Harley and an anonymous reviewer.

## References

- Balagansky, V.V., Timmerman, M.J., Kislitsyn, N.E., 2001. A 2.44 Ga syn-tectonic mafic dyke swarm in the Kolvitsa belt, Kola Peninsula, Russia: implications for early Palaeoproterozoic tectonics in the north-eastern Fennoscandian Shield. *Precambrian Research* 105, 269–287.
- Balagansky, V.V., Kaulina, T.V., Kislitsyn, R.V., 2005. The Kolvitsa mélange and the Umba terrane as a new type of structures of the Palaeoproterozoic Northeastern Baltic Shield. *Proceedings of Internat. Conference on Petrography of the XXI century*, vol. 1, pp. 139–141 (in Russian).
- Barbey, P., Raith, M., 1990. The granulite belt of Lapland. In: Vielzeuf, D., Vidal, Ph. (Eds.), *Granulites and Crustal Evolution*. Kluwer Publ., Dordrecht, pp. 111–132.
- Barbey, P., Convert, J., Martin, H., Capdevila, R., Hameurt, J., 1980. Relationships between granite-gneiss terrains, greenstone belts and granulite belts in the Archean crust of Lapland (Fennoscandia). *Geologische Rundschau* 69, 648–658.
- Bernard-Griffiths, J., Peucat, J.J., Postaire, B., Vidal, Ph., Convert, J., Moreau, B., 1984. Isotopic data (U–Pb, Rb–Sr Pb–Pb and Sm–Nd) on mafic granulites from Finnish Lapland. *Precambrian Research* 23, 325–348.
- Berthelsen, A., Marker, M., 1986. Tectonics of Cola collision suture and adjacent Archean and Early Proterozoic terrains in the northeastern region of the Baltic Shield (part 1). *Tectonophysics* 126, 31–55.
- Bibikova, E.V., Melnikov, V.F., Avakyan, K.Kh., 1993. Lapland granulites: petrology, geochemistry, isotopic age. *Petrology* 1 (2), 181–198 (Official English Translation).
- Bogdanova, S.V., 1996. High-grade metamorphism of 2.44–2.4 Ga age in mafic intrusions of the Belomorian Belt in the northeastern Baltic Shield. In: Bruwer, T.S. (Ed.), *Precambrian Crustal Evolution in the North Atlantic Region*. *Geol. Soc. Spec. Publ.*, vol. 112, pp. 69–90.
- Bridgwater, D., Scott, D.J., Balagansky, V.V., Timmerman, M.J., Marker, M., Bushmin, A., Alexeyev, N.L., Daly, J.S., 2001. Age and provenance of early Precambrian metasedimentary rocks in the Lapland–Kola Belt, Russia: evidence from Pb and Nd isotopic data. *Terra Nova* 13 (1), 32–37.
- Cherniak, D.J., 1993. Lead diffusion in titanite and preliminary results on the effects of radiation damage on Pb transport. *Chemical Geology* 110, 177–194.
- Daly, J.S., Balagansky, V.V., Timmerman, M.J., Whitehouse, M.J., de Jong, K., Guise, P., Bogdanova, S., Gorbatshev, R., Bridgwater, D., 2001. Ion microprobe U–Pb zircon geochronology and isotopic evidence for a trans-crustal suture in the Lapland–Kola orogen, northern Fennoscandian Shield. *Precambrian Research* 105, 289–314.
- Ellis, D.J., 1986. Garnet–liquid Fe<sup>2+</sup>–Mg equilibria and implication for the beginning of melting in the crust and subduction zones. *American Journal of Science* 286, 765–791.
- Fonarev, V.I., Graphchikov, A.A., 1991. Two-pyroxene thermometry: a critical evaluation. In: Perchuk, L.L. (Ed.), *Progress in Metamorphic and Magmatic Petrology. A Memorial Volume in Honor of D.S. Korzhinsky*. Cambridge University Press, pp. 65–92.
- Fonarev, V.I., Konilov, A.N., 2005. Pulsating evolution of metamorphism in granulite terrains: Kolvitsa meta-anorthosite massif, Kolvitsa Belt, northeast Baltic Shield. *International Geology Review* 47 (8), 815–850.
- Fonarev, V.I., Graphchikov, A.A., Konilov, A.N., 1991. A consistent system of geothermometers for metamorphic complexes. *International Geology Review* 33, 743–783.
- Fonarev, V.I., Graphchikov, A.A., Konilov, A.N., 1994. Experimental investigations of equilibria with minerals solid solutions and geological geothermobarometry. *Experimental Problems of Geology*. Nauka Press, Moscow, pp. 323–355 (In Russian).
- Frisch, T., Jackson, G.D., Glebovitsky, V.A., Yefimov, M.M., Bogdanova, M.N., Parrish, R.R., 1995. U–Pb ages zircon from the Kolvitsa gabbro–anorthosite complex, southern Kola Peninsula, Russia. *Petrology* 3 (3), 219–225 (Official English translation).
- Gaál, G., Gorbatshev, R., 1987. An outline of the Precambrian evolution of the Baltic Shield. *Precambrian Research* 35, 15–52.
- Gaál, G., Berthelsen, A., Gorbatshev, R., Kesola, R., Lehtonen, M.I., Marker, M., Raase, P., 1989. Structure and composition of the Precambrian crust along the Polar profile in the northern Baltic Shield. *Tectonophysics* 162, 1–25.
- Ganguly, J., Turone, M., 2001. Relationship between cooling rate and cooling age of a mineral: theory and applications to meteorites. *Meteoritics and Planetary Science* 36 (1), 167–177.
- Gerya, T.V., Perchuk, L.L., van Reenen, D.D., Smit, C.A., 2000. Two-dimensional numerical modeling of pressure–temperature–time paths for the exhumation of some granulite facies terrains in the Precambrian. *Journal of Geodynamics* 30, 17–35.
- Gerya, T.V., Maresch, W.V., Willner, A.P., van Reenen, D.D., Smit, C.A., 2001. Inherent gravitational instability of thickened continental crust with regionally developed low-to medium-pressure granulite facies metamorphism. *Earth and Planetary Science Letters* 190, 221–235.
- Gerya, T.V., Perchuk, L.L., Maresch, W.V., Willner, A.P., van Reenen, D.D., Smit, C.A., 2002. Thermal regime and gravitational instability of multi-layered continental crust: implications for the buoyant exhumation of high-grade metamorphic rocks. *European Journal of Mineralogy* 14, 687–699.
- Glebovitsky, V.A. (Ed.), 2005. *The Early Precambrian of the Baltic Shield*. Nauka Publishers, Saint-Petersburg. 711 p. (in Russian).
- Glebovitsky, V., Alexeyev, N., Marker, M., Bridgwater, D., Salmikova, E., Berezhnaya, N., 2001. Age, evolution and regional setting of the Palaeoproterozoic Umba igneous suite in the Kolvitsa–Umba zone, Kola Peninsula: constraints from new geological, geochemical and U–Pb zircon data. *Precambrian Research* 105, 247–268.
- Graphchikov, A.A., Fonarev, V.I., 1990. Garnet–orthopyroxene–plagioclase equilibrium and geobarometry, experimental study. In: Zharikov, V.A. (Ed.), *Experiment-89. Informative Volume*. Nauka Press, Moscow, pp. 34–37.
- Harley, S.L., 1989. The origin of granulites: a metamorphic perspective. *Geological Magazine* 126, 215–247.
- Harley, S.L., 1992. Proterozoic granulite terranes. In: Condie, K.C. (Ed.), *Proterozoic Crustal Evolution*. Elsevier, Amsterdam, pp. 301–359.
- Harris, L.B., Koyi, H., Fossen, H., 2002. Mechanisms for folding of high-grade rocks in extensional tectonic settings. *Earth-Science Reviews* 59, 163–210.
- Holdaway, M.J., Lee, S.M., 1977. Fe–Mg cordierite stability in high-grade pelitic rocks based on experimental, theoretical, and natural observations. *Contributions to Mineralogy and Petrology* 63, 175–198.
- Hörmann, P.K., Raith, M., Raase, P., Ackermann, D., Seifert, F., 1980. The granulite complex of Finnish Lapland: petrology and metamorphic conditions in the Ivalojokey–Inarijärvi area. *Bull. Geol. Surv., Finland*, vol. 308. 100 pp.
- Kaulina, T.V., Bogdanova, M.N., 1999. New U–Pb data on magmatic and metamorphic processes in the northwestern White Sea region. *Doklady Earth Sciences* 367 (5), 667–669 (Official English translation).
- Kaulina, T.V., Kislitsyn, R.V., Apanasevich, E.A., 2004. Final stages of the metamorphic evolution of the Tanaely belt, Kola Peninsula, Baltic Shield: evidence from U–Pb dating of zircon, titanite and rutile. *Geochemistry International* 42 (6), 513–520 (Official English translation).
- Kaulina, T.V., Belyaev, O.A., Apanasevich, E.A., 2005. Multistage metamorphic history of the Lapland Granulite and the Tanaely belts: U–Pb, Sm–Nd and Rb–Sr data (NE Baltic Shield). *Internat. Conf. on Precambrian Continental Growth and Tectonism*. (Abstract) February 22–24, 2005, Jhansi, India, 267–271.
- Kempton, P.D., Downes, H., Sharkov, E.V., Vetrin, V.R., Ionov, D.A., Carswell, D.A., Beard, A., 1995. Petrology and geochemistry of xenoliths from the Northern Baltic shield: evidence for partial melting and metasomatism in the lower crust beneath an Archean terrane. *Lithos* 36, 157–184.
- Kempton, P.D., Downes, H., Neymark, L.A., Wartho, J.A., Zartman, R.E., Sharkov, E.V., 2001. Garnet granulite xenoliths from the northern Baltic Shield — the underplated lower crust of a Palaeoproterozoic large igneous province? *Journal of Petrology* 42 (4), 731–763.
- Konilov, A.N., 1999. Testing of the consistent system of geothermometers and geobarometers of the program TPF. In: Zharikov, V.A. (Ed.), *Experiment in GeoSciences*, vol. 8, 1. Nauka Press, Moscow, pp. 60–62.
- Konilov, A.N., Graphchikov, A.A., Fonarev, V.I., Sultanov, D.M., 1997. A consistent system of geothermometers and geobarometers: testing with using independent experimental data. *Int. Meet. “Mineral Equilibria and Data Bases”*, Abstracts. *Espoo, Geol. Surv., Finland*, pp. 40–42.
- Kozioł, A.M., Newton, R.C., 1989. Grossular activity–composition relationship in ternary garnets determined by reversed displaced-equilibrium experiments. *Contributions to Mineralogy and Petrology* 103, 423–433.

- Kretz, R., 1983. Symbols for rock-forming minerals. *American Mineralogist* 68, 277–279.
- Krill, A.G., 1985. Svecofennian thrusting with thermal inversion in the Karasjok–Lävajok area of the northern Baltic Shield. *Norges Geologiske Undersøkelse* 403, 89–101.
- Lavrent'eva, I.V., Perchuk, L.L., 1981. Cordierite–garnet thermometer. *Doklady AN SSSR* 259 (3), 697–700 (in Russian).
- Ludwig, K.R., 1991. PBDAT program. US. Geol. Surv. Open-file Report, pp. 88–542. 38 pp.
- Ludwig, K.R., 1999. Isoplot/Ex, version 2.05, Berkeley Geochronology Center, Special Publication, 1a.
- Maaskant, P., 2004. Thermobarometry of the Furua granulites, Tanzania: a comparative study. *Neues Jahrbuch für Mineralogie. Abhandlungen*, Stuttgart 180, 065–100.
- Marker, M., 1985. Early Proterozoic (ca. 2000–1900 Ma) crustal structure of the northeastern Baltic Shield: tectonic division and tectogenesis. *Norges Geologiske Undersøkelse* 403, 55–74.
- Marker, M., Henkel, H., Lee, M.K., 1990. Combined gravity and magnetic modeling of the Tanaelv and Lapland granulite belts, northern Baltic Shield. *The European Geotraverse: Integrative Studies*. Eur. Sci. Found, Strasbourg, France, pp. 67–76.
- Marker, M., Kaulina, T.V., Daly, J.S., Kislitsyn, R., 1999. The Tanaelv belt and adjoining units in Finnmark, Norway, and in the western Kola Peninsula: State of knowledge from recent age isotopic and structural evidence. SVEKALAPKO, Europrobe Project. Abstract, Oulu, Finland, p. 77.
- Martignole, J., 1996. Tectonic setting of anorthositic complexes of the Grenville Province, Canada. In: Demaiffe, D. (Ed.), *Petrology and Geochemistry of Magmatic Suites of Rocks in the Continental and Oceanic Crust*. Bruxelles, Roy. Museum for Central, Africa, pp. 3–18.
- Melezhik, V.A., Sturt, B.F., 1994. General geology and evolutionary history of the Early Proterozoic Polmak–Pasvik–Pechenga–Imandra–Varzuga–Ust'Ponoy greenstone belt in the northeastern Baltic Shield. *Earth Science Reviews* 36, 205–241.
- Meriläinen, K., 1976. The granulite complex and adjacent rocks in Lapland, northern Finland. *Bulletin of the Geological Survey of Finland* 281 129 pp.
- Mezger, K., Rawnsley, C.M., Bohlen, S., Hanson, G.N., 1991. U–Pb garnet, sphene, monazite, and rutile ages: implications for the duration of the high-grade metamorphism and cooling histories. *Adirondack Mts. J. Geol.* 99, 415–428.
- Mints, M.V., Konilov, A.N., 1998. Thermal structure of the crust during granulite metamorphism: petrological speculations and geodynamic implications. *Origin and Evolution of Continents. Proceedings of Intern. Symp.*, Tokyo. Mem. Nat. Inst. of Polar Research. Spec. Issue, vol. 53, pp. 137–156.
- Mints, M.V., Konilov, A.N., 2004. Geodynamic crustal evolution and long-lived supercontinents during the Palaeoproterozoic: evidences from granulite–gneiss belts, collisional and accretionary orogens. In: Eriksson, P.G., Altermann, W., Nelson, D.R., Mueller, W.U., Catuneanu, O. (Eds.), *The Precambrian Earth: Tempos and events, series "Developments in Precambrian Geology, Condie, K.C. (Series ed.), 12"*. Elsevier, Amsterdam–Boston, pp. 223–239.
- Mints, M.V., Glaznev, V.N., Konilov, A.N., Kunina, N.M., Nikitichev, A.P., Raevsky, A.B., Sedikh, Yu.N., Stupak, V.M., Fonarev, V.I., 1996. The Early Precambrian of the northeastern Baltic Shield: Palaeogeodynamics, crustal structure and evolution. *Moscow, Scientific World*, 287 p. (Transactions of Geol. Inst. of Russ. Ac. Sci., v.503) (in Russian, with extended English abstract).
- Mitrofanov, F.P., Bayanova, T.B., 1999. Duration and timing of ore-bearing Palaeoproterozoic intrusions of Kola province. In: Stanley, R. (Ed.), *Mineral Deposits: Processes to Processing*. Balkema, Rotterdam, pp. 1275–1278.
- Mitrofanov, F.P., Balagansky, V.V., Balashov, Yu.A., Dokuchaeva, V.S., Gannibal, L.F., Nerovich, L.I., Radchenko, M.K., Ryungenen, G.I., 1995. U–Pb age of gabbro–anorthosite massifs in the Lapland Granulite Belt. *Norges Geologiske Undersøkelse, Special Publication* 7, 179–183.
- Nerovich, L.I., Zozulya, D.R., Kaulina, T.V., Delenizin, A.A., 2004. Initial magmas and conditions of an origin of anorthosites of the Lapland Granulite belt according to REE pattern and isotopes of Nd. *Materials of Internat. Sci.-Techn. Conf. "Science and Education - 2004"*, Murmansk, vol. 5. Murmansk State Techn. Univ., pp. 80–84 (in Russian).
- Neymark, L.A., Nemchin, A.A., Vetrin, V.R., Salnikova, E.V., 1993. Sm–Nd and Pb–Pb isotope systematics in deep crustal xenoliths and explosive pipes of the southern part of the Kola Peninsula. *Doklady Akademii Nauk* 326 (6), 781–784 (in Russian).
- Peltonen, P., Kontinen, A., Huhma, H., 1998. Petrogenesis of the mantle sequence of the Jormua ophiolite (Finland): melt migration in the upper mantle during Palaeoproterozoic continental break-up. *Journal of Petrology* 39 (2), 297–329.
- Perchuk, L., Gerya, T., 1989. Petrology and retrograde *P–T* path in granulites of the Kanskaya formation, Yenisey range, Eastern Siberia. *Journal of Metamorphic Geology* 7, 599–617.
- Perchuk, L.L., Lavrent'eva, I.V., 1983. Experimental investigation of exchange equilibria in the system cordierite–garnet–biotite. In: Saxena, S.K. (Ed.), *Kinetics and Equilibrium in Mineral Reactions. Advances in Physical Geochemistry*, vol. 3. Springer, Heidelberg–New York, pp. 199–239.
- Perchuk, L.L., Lavrent'eva, I.V., 1990. Some equilibria involving garnet, orthopyroxene and amphibole as geothermometers and geobarometers for metamorphic rocks. In: Zharikov, V.A. (Ed.), *Experiment-89, Informative Volume*. Nauka Press, Moscow, pp. 44–45.
- Perchuk, L.L., Krotov, A.V., Gerya, T.V., 1999. Petrology of the amphibolites of the Tana belt and the granulites of the Lapland complex. *Petrology* 7 (4), 339–365 (Official English translation).
- Powell, R., 1985. Regression diagnostics and robust regression in geothermometer/geobarometer calibration: the garnet–clinopyroxene geothermometer revised. *Journal of Metamorphic Geology* 3, 231–243.
- Raith, M., Srikantappa, C., Ashamanjari, K.G., Spiering, B., 1990. The granulite terrane of the Nilgiri Hills (Southern India): characterization of high-grade metamorphism. In: Vielzeuf, D., Vidal, Ph. (Eds.), *Granulites and Crustal Evolution*. Kluwer Ac. Publ., Dordrecht, pp. 339–365.
- Roberts, M.P., Finger, F., 1997. Do U–Pb zircon ages from granulites reflect peak metamorphic conditions? *Geology* 25 (4), 319–322.
- Sandiford, M., 1989. Horizontal structures in granulite terrain: a record of mountain building or mountain collapse? *Geology* 17, 449–452.
- Schumacher, R., Faulhaber, S., 1994. Summary and discussion of *P–T* estimates from garnet–pyroxene–plagioclase–quartz-bearing granulite facies rocks from Sri Lanka. *Precambrian Research* 66, 295–308.
- Sharov, N.V. (Ed.), 1997. *Seismological model of the lithosphere of Northern Europe: Lapland-Pechenga region*. Apatuty, Kola Science Centre, 226 p. (in Russian).
- Sneeringer, M., Hart, S.R., Shimizu, N., 1984. Strontium and samarium diffusion in diopside. *Geochimica et Cosmochimica Acta* 48 (8), 1589–1609.
- Sorjonen-Ward, P., Claeue-Long, J., Huhma, H., 1994. SHRIMP isotope studies of granulite zircons and their relevance to Early Proterozoic tectonics in northern Fennoscandia. *U.S. Geological Survey Circular* 1107 (ICOG 8) (Abstracts, 299).
- Stacey, J.S., Kramers, J.D., 1975. Approximation of terrestrial lead isotope evolution by a two-stage model. *Earth and Planetary Science Letters* 26, 207–221.
- Steiger, R.H., Jäger, E., 1976. Subcommittee on geochronology: convention of the use of decay constants in geo- and cosmochronology. *Earth and Planetary Science Letters* 36 (3), 359–362.
- Thompson, A.B., 1976. Mineral reactions in pelitic rocks. II Calculations of some *P–T–X* (Fe–Mg) phase relations. *American Journal of Science* 276, 425–454.
- Touret, J.L.R., Hartel, T.H.D., 1990. Synmetamorphic fluid inclusions in granulites. In: Vielzeuf, D., Vidal, Ph. (Eds.), *Granulites and Crustal Evolution*. Kluwer Publ., Dordrecht, pp. 397–417.
- Tuisku, P., Huhma, H., 2005. Generation of the norite–enderbite series of the Lapland Granulite Belt: implications from SIMS U–Pb-dating of zircons. *Geophysical Research Abstracts* 7, 08022.
- Vetrin, V.P., 1998. The Belomorian megablock lower crust: its age, structure and conditions of formation (by results of deep seated xenolith studying). *Proceedings of the Murmansk State Technical University* 1 (3), 7–18 (in Russian).
- Watson, E.B., Harrison, T.M., 1983. Zircon saturation revisited: temperature and composition effects in a variety of crustal magma types. *Earth and Planetary Science Letters* 64, 295–304.